Dissertation

submitted to the

Combined Faculties for the Natural Sciences and for Mathematics

Of the Ruperto-Carlo University of Heidelberg, Germany

For the degree of

Doctor of Natural Science

Presented by

M.Sc. Biomedical and Molecular Sciences, Sharavan Vishaan Venkateswaran

Born in: Chennai, India

Oral Examination: December 19th, 2017

Plk1 Overexpression Impairs Chromosome Segregation and Suppresses Tumor Development

Referees: Prof. Dr. Elmar Schiebel

Prof. Dr. Sylvia Erhardt

Acknowledgements

I would like to use this opportunity to express my heartfelt gratitude to everyone who aided me during this massive endeavor, without the continuous support and encouragement from the people around me this would have never been possible.

It has been a long journey wrought with moments of both triumph and frustration. Through all of it, my supervisor Rocio Sotillo has stood by me, never giving up on me even during my lowest points and I would like to show my appreciation for that dedication. I also want to thank her for providing me this opportunity to work in her lab and for guiding me over the past years. I am also extremely grateful to my TAC members Stefan Wiemann, Elmar Schiebel and Sylvia Erhardt for their valuable insights and feedback regarding my project.

Though it has evolved and changed a lot since the time of my joining, this lab has been like a home away from home. I would never forget all the past and present members who have helped me along the way. I would especially like to mention Joana Passos, Jose Paulo Lorenzo and Ana Maia who started out as colleagues and eventually became irreplaceable friends, without their support, I would not have reached the finish line. This section would be woefully incomplete without mentioning Konstantina Rowald who has been both a close friend and a mentor throughout this PhD from the beginning to the very end.

Furthermore, I want to convey my gratitude to all the members of the PhD council teams I was a part of as well as several friends and colleagues from DKFZ, Ploidynet and EMBL who have made this journey all the more exciting and memorable.

Special thanks to Hilary Davies-Rück, Lucie Wolf and Bianca Kuhn for helping me with the proofreading and German translations.

I am indebted to our collaborators Marcos Malumbres, Christopher Buccitelli, Nicholas McGranahan, Guillermo de Cárcer and Stephen Taylor for providing reagents as well as contributing to data acquisition and analysis. I am equally grateful to Simone Kraut, Kalman Somogyi and Jessica Steiner for unrivaled technical assistance. I am also thankful to Marko Lampe and the members of DKFZ microscopy facility for their help with experimental setup.

The Marie Curie Network Ploidynet which funded my research along with the DKFZ graduate school that supported me during my time as a PhD student both deserve my utmost recognition.

Last but definitely not the least, I want to thank my family and friends back home in India who have been patient with me over the last three years and supported me despite the limited time I had to offer them.

“Nothing in life is to be feared, it is only to be understood. Now is the time to understand more, so that we may fear less.”

— Marie Curie

Summary

Polo-like kinase 1 (Plk1) is a serine-threonine protein kinase widely accepted as one of the master regulators of cell cycle. Overexpression of Plk1 is a frequent occurrence in an array of different human tumor types and it is usually correlated with poor prognosis in patients. However, very little is known about the exact role of Plk1 in tumorigenesis. Here, we use inducible mouse models to determine the *in vivo* consequences of Plk1 overexpression. During this study, we established that Plk1 is not an oncogene and overexpression of Plk1 has a strong tumor suppressive effect on Her2 or Kras driven breast cancer. Furthermore, tumors with elevated levels of Plk1 displayed evidence of whole genome doubling coupled with increased levels of aneuploidy. Histological characterization of murine mammary glands prior to tumor development affirmed a correlation between Plk1 overexpression and increase in genomic content at an early stage. Utilizing *in vitro* culture systems, we demonstrate that overexpression of Plk1 leads to reduced proliferation and causes polyploidy. Time-lapse imaging of mammary organoid cultures and mouse embryonic fibroblasts (MEFs) overexpressing Plk1 revealed that the polyploid cells originate due to impaired chromosome segregation as well as a failure of cytokinesis occurring during mitosis. Increased mitotic aberrations and supernumerary centrosomes accompanied these defective cell division processes. Mechanistically, the observed phenotype can be partially attributed to decrease of Shugoshin 1 (Sgo1) a target of Plk1, which is responsible for maintaining cohesion at the centromeres thus holding the sister chromatids together prior to anaphase. Premature loss of Sgo1 during prometaphase caused a partial or complete loss of cohesion.

In this dissertation, we report that one of the major consequences of Plk1 overexpression is a staggering tumor suppressive effect, although this does not necessarily negate the possibility that Plk1 could promote tumor development under a different set of circumstances. Despite these findings, Plk1 inhibition in human tumors could still have a beneficial outcome because the kinase is indispensable for cell division. This work is not aimed at discouraging further research on Plk1 inhibitors; rather it provides a testament to the use of genetically engineered mouse models (GEMMs) that closely mimic human disease for pre-clinical testing. It is imperative to understand the molecular mechanisms and cellular processes leading up to tumor onset prior to the development of therapeutic strategies.

Zusammenfassung

Nach allgemeiner Auffassung ist die Serin/Threonin-Proteinkinase Polo-like-Kinase 1 (dt. "Polo-ähnliche Kinase 1", Plk1) eine der Hauptregulatoren des Zellzyklus. Überexpression der Plk1 ist ein häufiges Merkmal verschiedener Tumorarten und korreliert in Patienten normalerweise mit einer schlechten Prognose. Die genaue Funktion der Plk1 während der Tumorentwicklung ist allerdings nur unzureichend bekannt. In dieser Arbeit untersuchen wir die Konsequenzen der Plk1 Überexpression in vivo mit Hilfe von induzierbaren Mausmodellen.

Wir konnten feststellen, dass Plk1 nicht als Onkogen agiert, sondern das die Überexpression von Plk1 vielmehr eine stark tumorsuppressiven auf Her2- oder Kras-positiven Brustkrebstypen hat.

Des Weiteren waren Plk1-überexprimierende Tumoren sowohl durch eine Verdopplung des kompletten Genoms als auch ein verstärktes Auftreten von Aneuploidie gekennzeichnet. Histologische Untersuchungen der murinen Brustdrüsen noch vor der Tumorentstehung bestätigten schon in diesem frühen Stadium einen Zusammenhang zwischen der Überexpression von Plk1 und erhöhtem Genomgehalt.

Durch den Einsatz von in vitro Kultursystemen konnten wir nachweisen, dass Überexpression der Plk1 zu Polyploidie und einer verringerten Proliferation führt. Darüber hinaus konnten wir durch Zeitraffer-Mikroskopie (engl. time-lapse imaging) von Organoidkulturen aus Brustgewebe und murinen embryonalen Fibroblasten (MEFs) mit Plk1 Überexpression zeigen, dass die polyploiden Zellen aufgrund von Fehlern während der Mitose entstehen, etwa bei der Trennung der Chromosomen oder der Zytokinese. Diese fehlerhaften Zellteilungen traten zusammen mit einer erhöhten Anzahl mitotischer Anomalien und überzähliger Chromosomen auf.

Der beobachtete Phänotyp lässt sich mechanistisch teilweise durch eine Verminderung des Shugoshin 1 (SGO1) Proteingehaltes an den Kinetochoren erklären. Dieses Protein ist für den Zusammenhalt der Zentromeren und damit für das Zusammenbleiben der Schwesterchromatiden vor der Anaphase verantwortlich. Der zu frühe Verlust von SGO1 schon während der Prometaphase führte teilweise oder vollständig zum Verlust dieses Zusammenhaltes.

In dieser Doktorarbeit zeigen wir den stark tumorsuppressiven Effekt als eine der bedeutendsten Konsequenzen von Plk1 Überexpression, wobei dies nicht zwangsläufig die Möglichkeit ausschließt, dass Plk1 unter anderen Umständen die Tumorentwicklung begünstigen könnte. Trotz dieser Ergebnisse könnte auch eine gegen Plk1 gerichtete Behandlung von humanen Tumoren eine vorteilhafte Wirkung haben, weil die Plk1 unverzichtbar für die Zellteilung ist.

Diese Arbeit hat nicht das Ziel, von jeglichen weiteren Bemühungen zur Blockade der Plk1 abzuraten. Vielmehr soll sie den Nutzen von genetisch veränderten Mausmodellen (engl. genetically engineered mouse models, GEMMs) für die präklinische Forschung hervorheben, die humane Krankheiten präzise nachahmen. Es ist zwingend notwendig, die molekularen Mechanismen und zellulären Prozesse der Tumorentstehung zu verstehen, bevor man Therapiestrategien entwickelt.

Table of Contents

Abbreviations

Numbers

3D	Three Dimensional

A

AKT	Protein Kinase B
AMP	Amplification
APC	Anaphase Promoting Complex
ATM	Ataxia Telangiectasia Mutated
ATR	Ataxia Telangiectasia and Rad3-related

B

BRCA1/2	Breast Cancer 1/2
Bub1	Budding Uninhibited by Benzimidazol 1
BubR1	Budding Uninhibited by Benzimidazol Related 1
BWA	Burrows-Wheeler Aligner

C

C57BL/6J	C57 black 6
Cdk	Cyclin Dependent Kinase
cDNA	Complementary DNA
Cep55	Centrosomal protein of 55 kDa
CIN	Chromosomal Instability
ColA1	Collagen, type I, alpha 1
Ctrl	Control

D

DAPI	4’,6-Diamidin-2-Phenylindol
DEL	Deletion
dH2O	Destilled Water
DMEM	Dulbecco's Modified Eagle Medium
DNA	Deoxyribonucleic Acid
dNTP	Deoxynucleoside triphosphate
Dox	Doxycycline

E

E1A	Adenovirus early region 1A
EGFR	Epidermal Growth Factor Receptor
EHS	Engelbreth-Holm-Swarm
EMBL	European Molecular Biology Laboratory
ERBB2	Erythroblastosis Oncogene B 2
ER	Estrogen Receptor
ES cells	Embryonic Stem cells
ESCRT	Endosomal sorting complexes required for transport

F

FOV	Field of view
FVB	Sensitive to Friend Leukemia Virus B strain

G

G-phase	Gap phase
GCR	Gross Chromosomal Rearrangement
GEF	Guanine nucleotide exchange factor
GEMMs	Genetically Engineered Mouse Models
GTPase	Guanosintriphosphatase

H

H2B-GFP	Histone 2B-Green Fluorescent Protein
HCl	Hydro Chloric acid
Her2	Human Epidermal Growth Factor Receptor 2
HRasV12	Harvey Rat Sarcoma Viral Oncogene Homolog

I

IgG	Immunglobuline G

K

KCl	Potassium chloride
KD	Kinase Domain
K-MT	Kinetochore-Microtubule
Kras	Kirsten Rat Sarcoma Viral Oncogene Homolog

M

M-phase	Mitosis phase
Mad2	Mitotic Arrest Deficient 2
MAPK	Mitogen Activated Protein Kinase
MEBM	Mammary Epithelial Cell Basal Medium
MEFs	Mouse Embryonic Fibroblasts
I-FISH	Interphase Fluorescence In Situ Hybridization
MMTV	Mouse Mammary Tumor Virus

N

NaOH	Sodium hydroxide
NEBD	Nuclear Envelope Breakdown
Nlp	Ninein-like protein
n.s.	Not significant

P

p	Phospho/Phosphorylated
PBS	Phosphate Buffered Saline
PBD	Polo-Box Domain
PCG	Partial Chromosome Gain
PCL	Partial Chromosome Loss

PCR	Polymerase Chain Reaction
pH3	phospho Histone 3
PI3K	Phosphatidylinositol-4,5-bisphosphate 3-kinase
Plk1	Polo-like Kinase 1
PR	Progesterone Receptor

R

RhoA	Ras homolog gene family, member A
RIPA	Radioimmunoprecipitation Assay
RNA	Ribonucleic Acid
RT	Room Temperature
RT-qPCR	Reverse Transcriptase quantitative Polymerase Chain Reaction
rtTA	Reverse Tetracycline Transactivator

S

S-phase	Synthesis phase
SAC	Spindle assembly checkpoint
SCNA	Somatic Copy Number Alteration
Sgo1	Shugoshin 1
SDS	Sodium Dodecyl Sulfate

T

T210/Thr210	Threonine 210
TBS-T	Tris Buffered Salin with Tween20
TEMED	Tetramethylethylendiamine
Tet	Tetracycline
tTA	Tetracycline Transactivator
TUNEL	TdT-mediated dUTP-biotin nick end labeling

W

WCG	Whole Chromosome Gain
WCL	Whole Chromosome Loss

Introduction

Polo-like Kinase 1 (Plk1)

1.1 Plk1 Discovery, Structure and Function

Polo-like kinase is a serine threonine protein kinase, ordained as one of the master regulators of cell cycle. The gene encoding for Plk1 was first discovered over forty years ago in yeast, by screening for mutants defective in cell division (Hartwell *et al.*, 1973). Plk1 gets its unique name because cells lacking this kinase display a strong tendency to form a monopolar spindle with the chromosomes arranged in a circular manner resembling the shape of a Polo. This was first observed in *Drosophila* (Sunkel and Glover, 1988). In humans, Plk1 is a conserved member of a family of four related kinases, each with varied yet unrelated functions (Van De Weerdt and Medema, 2006).

The protein is composed of 603 amino acids and structurally it includes a kinase domain (KD) at the N-terminal plus two conserved regions termed as polo-box domains (PBD) located at the C-terminal (Fig1.1). While the kinase domain is essential for the functional activity of the kinase, the PBDs are responsible for mediating subcellular localization, protein interactions as well as exertion of partial control over the N-terminal kinase activity (Cheng *et al.*, 2003).

a

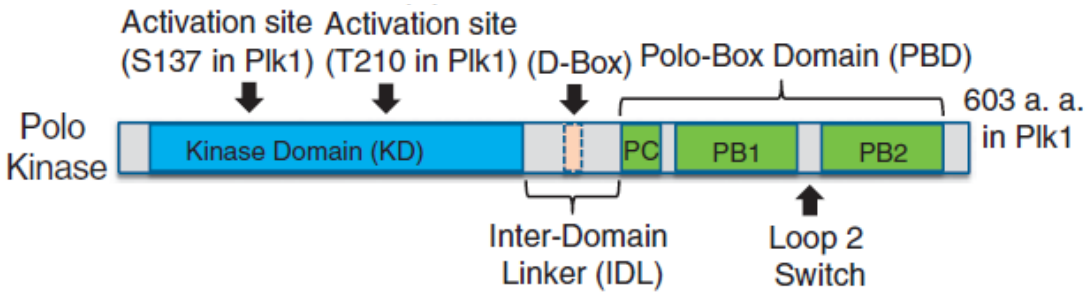

b

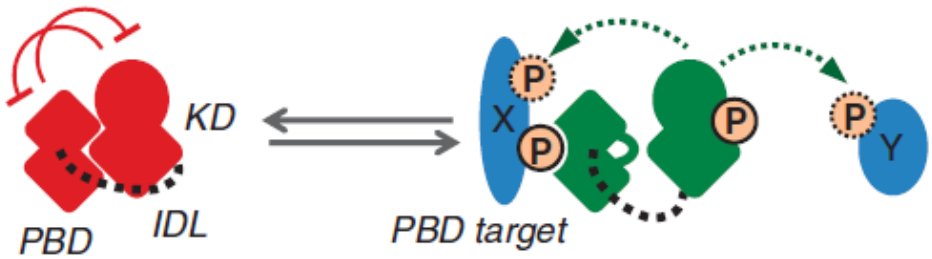

Fig1.1: (a) Basic structure of Plk1 showing the PBD at the C-terminal and KD at the N-terminal. (b) Schematic of Plk1 activity (Archambault, Lépine and Kachaner, 2015).

The basic functioning of the kinase is illustrated by the simple schematic shown above (Fig1.1b). The polo-box domain recognizes and binds to a protein (X) that has been primed by another kinase via phosphorylation at a certain site, following which the kinase domain of Plk1 can then phosphorylate the same protein at another motif or interact with a separate protein (Y) in the region. The KD and PBD can also inhibit each other via intramolecular interaction. This mode of action allows for Plk1 to change localization and to exert considerable amount of control over several different targets during mitotic progression (Lee *et al.*, 1998; Archambault, Lépine and Kachaner, 2015).

1.2 Mitotic regulation by Plk1

Plk1 is regarded to be just as important as the Cyclins and Cdks when it comes to mitotic regulation. The roles of Plk1 in mitosis range from transition of G2 into M phase all the way up to cytokinesis. One of the most interesting aspects of Plk1 is the ability to change subcellular localization as per functional needs during cell division; the mechanism by which the kinase achieves this feat was discussed in the previous section. The localization of Plk1 at different phases of mitosis and its broad functions are shown in Fig1.2. Activation of Plk1 is achieved by the phosphorylation at the T-loop (Thr210) by Aurora kinase at the start of the G2 phase, it is also important to note the co-factor Bora is essential for this step (Seki, Coppinger and Jang, 2008).

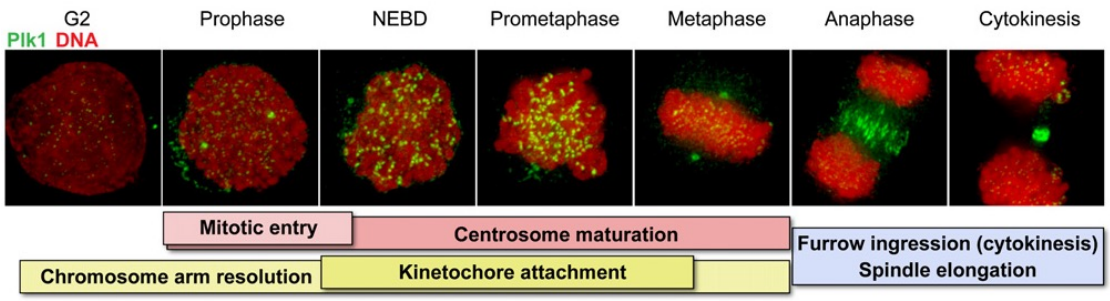

Fig1.2: Functions and localization of Plk1 (green) during different phases of mitosis (Petronczki, Lenart and Peters, 2008).

Once activated, Plk1 localizes at the centrosomes and facilitates transition from G2 to M by phosphorylation of cyclin B1 facilitating its translocation into the nucleus thereby signaling the start of mitosis (Toyoshima-Morimoto *et al.*, 2001). One of the most important functions of Plk1 during prophase is centrosome maturation, which is in turn a prerequisite for nucleation of microtubules and the subsequent formation of the spindle. Plk1 assists in centrosome maturation by phosphorylation of centrosomal protein Nlp, which indirectly facilitates the recruitment of γ tubulin complexes to the centrosome (Casenghi M, Meraldi P, Weinhart U, Duncan PI, Körner R, Nigg, 2003).

Following nuclear envelope breakdown (NEBD) there is an increase in Plk1 levels at the kinetochores; this has been mainly attributed to mediating kinetochore-microtubule (K-MT) attachment, since the strong staining is observed up until alignment of the chromosomes. Studies have verified the link Plk1 shares with the spindle assembly checkpoint (SAC), confirming the presence of increased levels of the protein at unattached kinetochores. The SAC is primarily responsible for preventing transition into anaphase till all kinetochores are attached to the spindle. Furthermore, one of the targets of Plk1 during this phase is BubR1 an important component of the SAC. It has been proven that this phosphorylation of BubR1 is essential for maintaining the stability of K-MT attachments (Elowe *et al.*, 2007).

Plk1 also partakes in the disruption of sister chromatid cohesion prior to anaphase; this will be discussed elaborately in the following section. Early studies describing the functions of Plk1 were performed by complete inhibition or knockouts, this inadvertently led to the SAC mediated arrest of these cells at prometaphase (Sunkel and Glover, 1988; Kishi *et al.*, 2009). Hence much was not known about the functions of Plk1 during anaphase and telophase, however the localization of the protein at the middle of the spindle in anaphase suggests a role in mediating the formation of the cleavage furrow and cytokinesis. Recent studies have been able to show that Plk1 indeed has a vital function in cytokinesis (Burkard *et al.*, 2007; Kim *et al.*, 2014), this is explained in more detail in the upcoming sections.

1.3 Plk1 and Cohesion

Cohesion in this case refers to the protein complex that holds the sister chromatids together before the start of anaphase. It is also responsible for the typical X shaped appearance of the chromosomes. Majority of the cohesion is removed from the chromatin early on in mitosis to allow the formation of the sister chromatids, however cohesion is still retained mainly at the centromeres (Losada, Hirano and Hirano, 2002). This cohesion complex is protected by another protein Shugoshin 1 (Sgo1) also dubbed as the guardian of cohesion (Kitajima *et al.*, 2006), which is recruited to the centromere at the late G2 phase (Perera and Taylor, 2010).

Plk1 affects cohesion by a twofold mechanism, first it phosphorylates Sgo1 effectively removing it from its centromeric localization prior to anaphase (Shintomi and Hirano, 2010). Plk1 also directly phosphorylates cohesion subunits SA2 and Scc1. Phosphorylation of the SA2 subunit results in reduced affinity to chromatin, which is essential for the removal of cohesion from the arms following prophase (Fig1.3). While the phosphorylation of Scc2 assists cohesion cleavage by Separase during the transition from metaphase to anaphase (Hornig and Uhlmann, 2004).

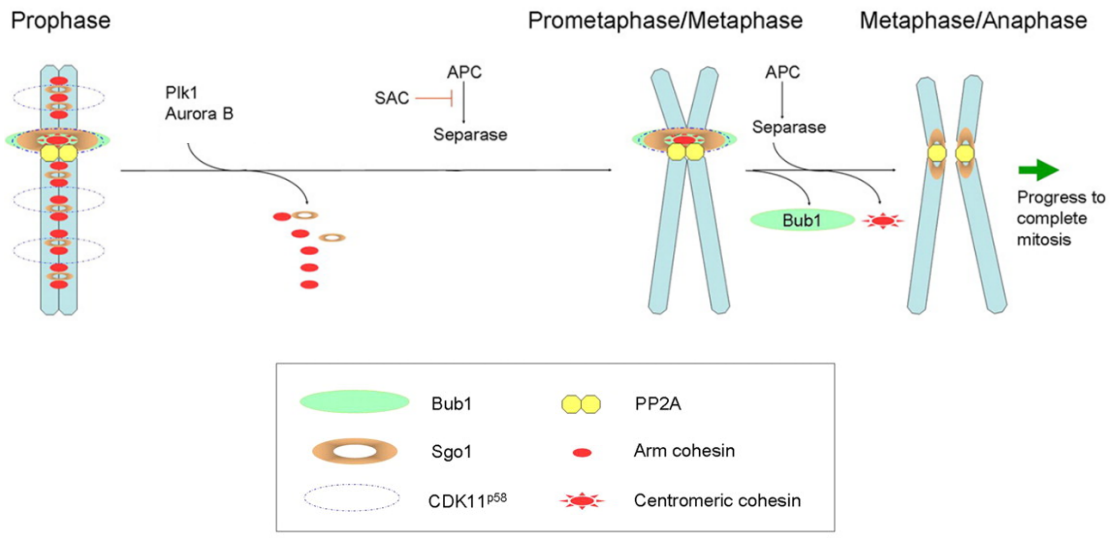

Fig1.3: Schematic diagram displaying maintenance of cohesion till anaphase. Plk1 mediated phosphorylation is responsible for displacing centromeric Sgo1 and releasing arm cohesion (Hu *et al.*, 2007).

1.4 Cytokinesis and the roles of Plk1

The final stage of mitosis, which results in two independent daughter cells, is called cytokinesis. This process is initiated at the end of anaphase and it is marked by the formation of a cleavage furrow in between the separated nuclear material. The ingression of the cleavage furrow is controlled by an actin-myosin contractile ring. There are two essential steps leading to successful cytokinesis, the first is the formation of the contractile ring at the start of the process and the second is the assembly of the abscission complex at the end of the process. Plk1 is linked to both these mandatory steps.

The formation and functioning of the contractile ring requires the accumulation and activation of the RhoA GTPase at the equatorial cortex. Although Plk1 is not essential for the recruitment of RhoA, it was shown that Plk1 was required for the proper localization of important RhoA activation factor, the GEF protein Ect2 (Burkard *et al.*, 2007; Petronczki, Lenart and Peters, 2008).

For abscission to occur properly at the end of cytokinesis, the ESCRT complex must be assembled. The localization of the protein Cep55 to midbody after the end of anaphase triggers this process. The phosphorylation of Cep55 by Plk1 prevents the premature localization to the midbody, effectively controlling the timing of abscission (Carmena, 2012). Thus, Plk1 exerts control over the start and end of cytokinesis.

1.5 Plk1 and CIN in Tumors

Chromosomal instability (CIN) is one of the prominent hallmarks of human cancer, which is linked with poor patient survival. It is an ongoing process by which either whole or parts of chromosomes are gained or lost. CIN is known to promote tumor evolution and drives resistance to therapy (Godek *et al.*, 2016; Rowald *et al.*, 2016; López-García *et al.*, 2017). Overexpression of certain genes are commonly associated with CIN, this is aptly dubbed as the CIN70 signature (Carter *et al.*, 2006). Most of these genes control vital processes occurring during cell division. As such overexpression of the individual genes that are a part of the CIN70 in an experimental context lead to spontaneous tumor initiation (Sotillo *et al.*, 2007; Nam and Van Deursen, 2014). Plk1 is also a part of this infamous CIN70 gene signature.

Overexpression of Plk1 is a common occurrence observed in several different types of human tumors and it usually correlates with bad prognosis in patients (Eckerdt, Yuan and Strebhardt, 2005). Plk1 overexpression has also been implicated to play an early stage role in the development of certain carcinomas (Ito *et al.*, 2004). Furthermore, Plk1 is a known antagonist of the prominent tumor suppressor p53 (Ando *et al.*, 2004; Liu *et al.*, 2010).

Considering these factors plus the importance of Plk1 in cell division and adding to this the fact that it is an easily druggable kinase, all make it an attractive target for anticancer therapy. Hence this has led to the development of several small molecule inhibitors for Plk1, among these BI2536 is known to inhibit Plk1 with higher specificity and is considered for treatment against leukemia and non-small cell lung cancer (Lénárt *et al.*, 2007; Steegmaier *et al.*, 2007; Medema, Lin and Yang, 2011; Choi *et al.*, 2015; Gutteridge *et al.*, 2016).

Despite reasonable success using this inhibitor, the causative role of Plk1 in tumorigenesis is still under debate. Due to the highly proliferative nature of the tumors and the fact that Plk1 levels are cell cycle dependent, it has been argued that Plk1 overexpression is merely a consequence of increased proliferation caused by oncogenic transformation (Cholewa, Liu and Ahmad, 2013). The role of Plk1 in neoplastic transformation and tumor development has yet to be completely deduced.

Cancer

1.6 Whole Genome Doubling in Tumorigenesis

According to recent studies, a staggering 20% of all human tumors display near tetraploid karyotypes and whole genome doubling events during tumor development have occurred in roughly 37% of tumors, including those with a near diploid karyotype (Dewhurst *et al.*, 2014). Tetraploid cells, directly resulting from

genome doubling events have been observed in early stages of solid tumors even in very preliminary histological studies (Kirkland, 1966). A p53 dependent mechanism is usual in place to halt the proliferation of these potentially oncogenic tetraploid cells (Ganem and Pellman, 2007).

Tetraploidization in a tumor context can be caused by several independent events, prominent among them are faulty chromosome segregation due to mitotic defects or cytokinesis failure, cell fusion and chromosome endoreduplication (Fig1.4). Cytokinesis failure in p53 deficient cells is enough to promote tumorigenesis whereas in p53 proficient cells it leads to the activation of the Hippo tumor suppressor pathway (Fujiwara *et al.*, 2005; Ganem *et al.*, 2014). Surprisingly, even tumors with an intact p53 function can undergo genome doubling and maintain a tetraploid karyotype. This is due to a mechanism of tolerance driven by cyclin D overexpression at the early stages of tumor development (Crockford *et al.*, 2017).

Whole genome doubling has also been shown to be a prominent driver of cancer genome evolution by promoting CIN. Tetraploid cells demonstrate a better tolerance towards chromosomal aberrations, which allows for the accumulation of several genetic alterations over time, eventually leading to tumorigenesis or development of resistant clones (Dewhurst *et al.*, 2014).

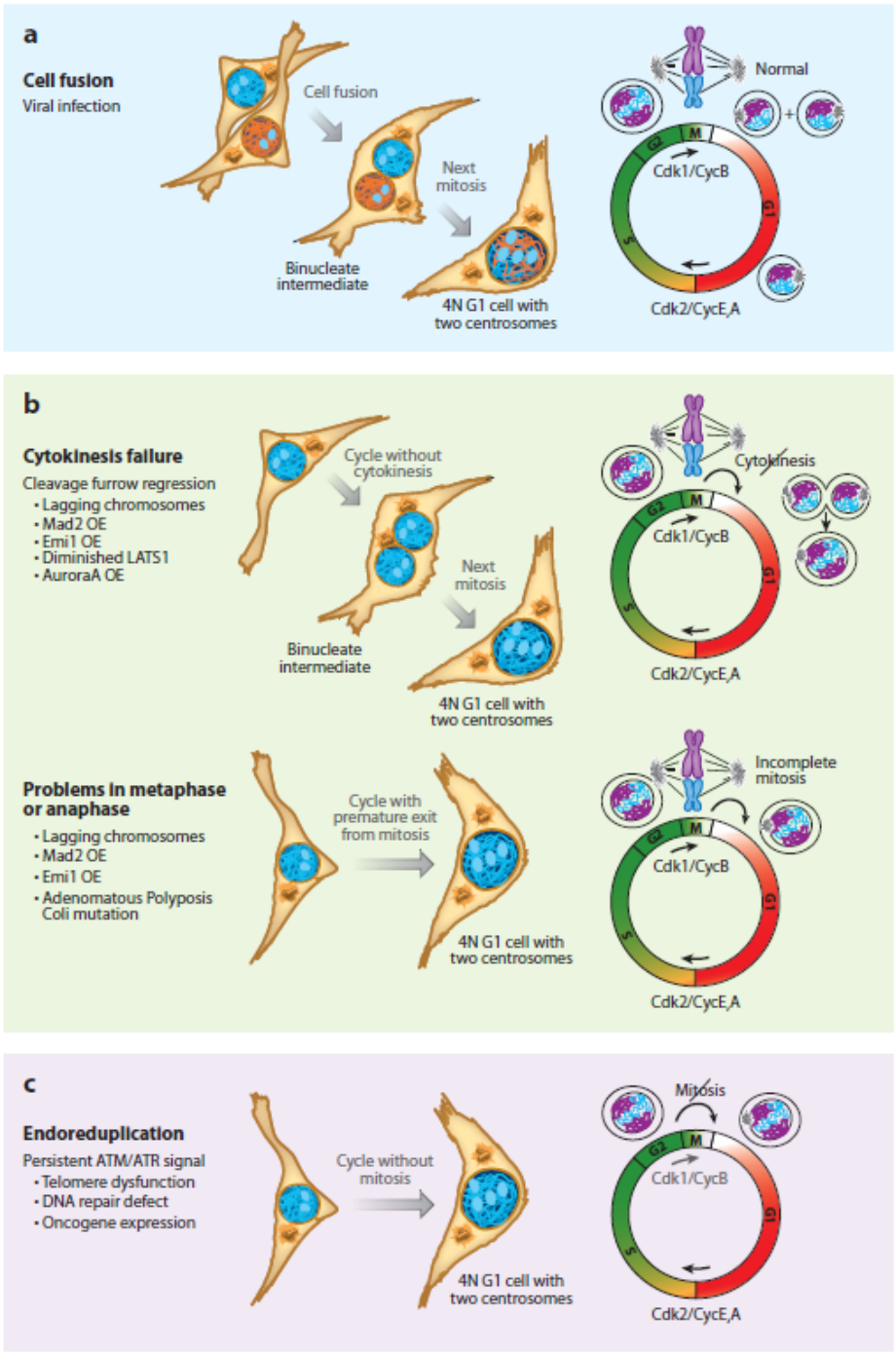

Fig1.4: Schematic showing the main mechanisms of tetraploidization in tumors and the causative factors for each mechanism. "Abbreviations: ATM/ATR, ataxia telangiectasia mutated/ATM and Rad3-related; Cdk, cyclin-dependent kinase; Cyc, cyclin; LATS1, large tumor suppressor 1; Mad2, mitotic arrest deficient 2; OE, overexpression." (Davoli, de Lange and Lange, 2011).

1.7 Breast Cancer

Breast cancer is responsible for one of the highest cancer related mortality rates in women worldwide. Besides the usual cancer risk factors, women who are post menopause, had children late and those who underwent hormone replacement therapy have a higher risk of breast cancer (Siegel, Miller and Jemal, 2015). Hence

specific screening of females of the age group 40-70 has proven to be beneficial, helping early detection of the disease (Nelson *et al.*, 2009). Approximately 5-10% of all breast cancer cases are also attributed to inherited genetic traits, this includes mutations in BRCA1 and BRCA2. The five-year survival rate of women diagnosed with breast cancer in developed countries is as high as 80-90%, however the disease still claimed the lives of 522,000 women worldwide in the year 2012 (World Cancer Report 2014).

Most breast cancer related mortality is not due to the primary tumor but caused by metastasis of the tumor cells mainly to the lung, brain or the bone. Early detection of the disease is paramount in stopping metastasis. Breast cancer is detected mainly by mammography and the diagnosis is confirmed by the biopsy of the abnormal growth (Nelson *et al.*, 2009). Once detected, the normal mode of treatment is surgical removal of the tumor and the surrounding region. This is accomplished either by lumpectomy which is the removal of a small region of the breast or the entire breast is removed by mastectomy. The exact surgical procedure is determined on a case-by-case basis based on the size and staging of the tumor. The treatment takes a multidisciplinary approach to reduce the chance of remission, therefore surgery is usually followed by radiotherapy, chemotherapy, hormone-blocking therapy or targeted therapy (Saini *et al.*, 2012). The second line treatment is determined primarily by the receptor status of the tumor, deduced by immunohistochemistry of the tumor biopsy. If the cancer cells express the estrogen receptor (ER) or progesterone receptor (PR), since they depend on that hormone for their proliferation, they can be treated using drugs that block the effect on the hormone (Burstein *et al.*, 2014). A good example of this is the treatment of ER positive tumors with tamoxifen. The tumors that are positive for the Her2 receptor can be treated with trastuzumab which is a monoclonal antibody or lapatinib which is a tyrosine kinase inhibitor (Moasser and Krop, 2015; Goel *et al.*, 2016).

The breast is also one of the tissues that is most susceptible to cancer due to the constant cycles of cell proliferation and death driven by the hormonal fluctuations of the estrous cycle (Visvader and Stingl, 2014). The high rate cell turnover increase the chance of chromosomal aberrations or erroneous DNA replication, thereby also increasing cancer risk (Ashford *et al.*, 2015).

1.8 Modelling Breast Cancer in Mice

Genetically engineered mouse models (GEMMs) are a valuable resource for dissecting the molecular mechanisms behind tumorigenesis. A necessary solution to circumvent the limitations of studies using primary patient material. By closely mimicking the human disease, GEMMs allow us to study tumor initiation, progression and provide a platform to test new treatment methods (Menezes *et al.*, 2014).

There are many approaches for the development of transgenic mouse models, one of the most prevalent methods is the random integration of the gene of interest into the germline of the mouse, achieved by injecting the DNA directly into the pronuclei of the fertilized egg (Cho, Haruyama and Kulkarni, 2009). This method was used to identify potential oncogenes and drivers of breast cancer by utilizing the breast tissue specific MMTV (mouse mammary tumor virus) promoter to control transcription (Wang *et al.*, 1994). Since some of these genes proved to be embryonic lethal and owing to the fact that breast cancer is mainly a disease observed in adults of the species, it also became essential to control the timing of induction of these genes. This conundrum led to the development of mouse models with the possibility to selectively induce expression of the transgene in a time-controlled manner. The most prominent among these models is the tetracycline inducible system (Tet-ON/Tet-OFF). The mode of action of this system is described in figure1.5 shown below. Thus, the MMTV-rtTA and MMTV-tTA systems were established to selectively induce the expression of transgenes in the mammary glands and monitor their oncogenic potential (Boxer *et al.*, 2004).

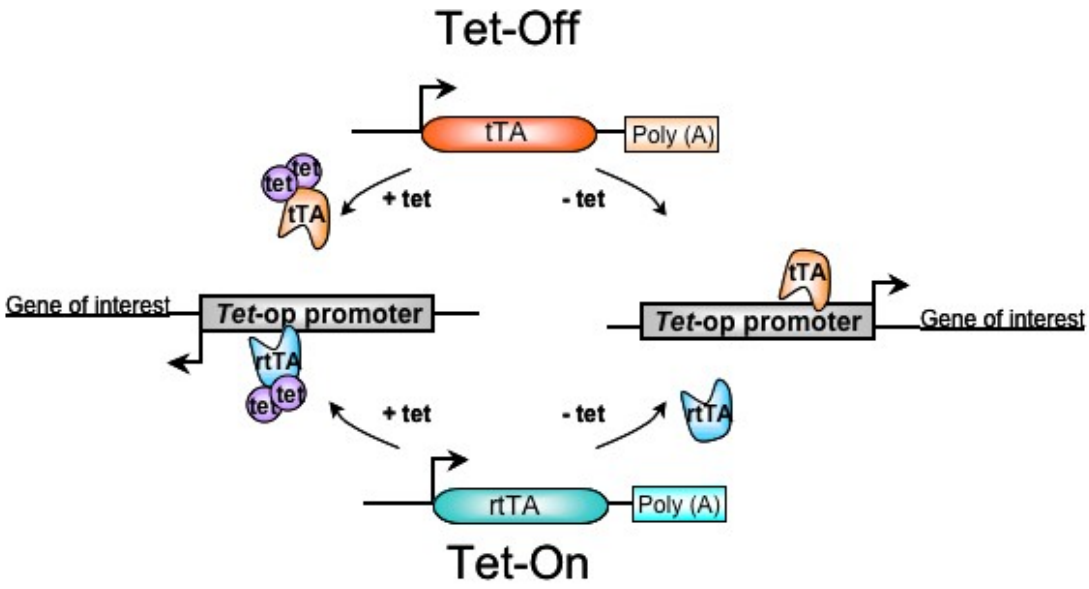

Fig1.5: Tetracycline inducible system and the mode of operation. Tet-ON: The expression of the transgene is induced in the presence of tetracycline or its analog doxycycline. Tetracycline binds to the transcription factor rtTA this in turn binds to the promoter region inducing gene expression. Tet-OFF: Expression of transgene is inhibited in the presence of tetracycline or its analog. Tetracycline binds to transcription factor tTA preventing its association with the promoter region, effectively switching off gene expression. Figure source: https://www.genoway.com.

Due to the sheer number of different mouse models currently in use to study cancer, I will limit the rest of this section only to briefly describe those models, which are relevant for understanding this project.

Overexpression of the Her2 receptor due to the amplification of the corresponding gene ERBB2 is prevalent in 25% of all cases of human breast cancer. Her2 is a

member of the EGFR receptor family and is as such responsible for promoting proliferation and survival by downstream signaling through MAPK and PI3K-AKT pathways respectively (Rexer and Arteaga, 2012). The conditional overexpression of Her2 using a tetracycline-inducible mouse model system, led to the development of mammary tumors in the entire colony, with an average latency of 42 days. Oncogene withdrawal by removal of doxycycline, caused the complete regression of tumors in all the animals, however relapse of the tumor was observed in 64% of the animals several months post treatment (Moody *et al.*, 2002).

Although the Ras family of genes is frequently mutated in cancer (32%), it is only observed to be the case in 7% of breast cancer patients with Kras mutations contributing to 4% of the cases (O'Hagan and Heyer, 2011; Pylayeva-Gupta, Grabocka and Bar-Sagi, 2011). This can be attributed to the frequently observed overexpression of Her2 in breast cancer. Since Her2 is upstream of Ras in the same pathway, cancer cells have no further requirement to modify this pathway (Pylayeva-Gupta, Grabocka and Bar-Sagi, 2011). Even though Kras mutations are a relatively minor occurrence in breast cancer, nevertheless a tetracycline inducible mouse model was developed to study Kras as a driver of mammary tumorigenesis. These mice developed mammary tumors with an average latency of 154 days (Podsypanina *et al.*, 2008).

In vitro Model Systems

1.9 Mammary Organoids

The advent of mouse models has provided us with a valuable tool for studying the events that lead to transformation. However, understanding certain cellular processes is beyond the scope of just utilizing mouse model systems. Traditional cell culture techniques do not provide an accurate representation of the in vivo organism and this has led to the development of 3-dimensional culture systems.

3D organotypic culture systems or organoids have been utilized to study cell-cell interactions, tissue development, signaling as well as effect of drugs. These 3D cultures can be established from single epithelial cells obtained from various tissues (Shamir and Ewald, 2014). In a normal mammary gland, cells differentiate to form acini and ducts which are responsible for milk production and delivery (Visvader and Stingl, 2014). To recapitulate this process *in vitro*, extra cellular matrix molecules with basement membrane proteins are required. Matrigel, which is a gelatinous membrane protein secreted by EHS mouse sarcoma cells is commonly utilized as a substitute to fulfil this requirement. When single mammary epithelial cells are seeded in Matrigel, they develop to form hollow spherical structures which closely resemble the mammary gland acini (Petersen *et al.*, 1992).

A new approach for studying the effects of oncogenic transformation *in vitro* combines MMTV-rtTA tetracycline inducible mouse models and organotypic culture systems. Using mammary cells from these mouse models to develop organoids, an inducible *in vitro* system to monitor the effects of oncogene induction over time, has been established. With the induction of the oncogenes, epithelial cells loose polarity and the rapidly dividing cells eventual lead to the filling up of the hollow acini-like spheres. These events closely mimic the progression of invasive ductal carcinoma in humans (Jechlinger, Podsypanina and Varmus, 2009).

Objectives

This work was primarily conceived to investigate the *in vivo* consequences of Plk1 overexpression during tumorigenesis. We utilized inducible GEMMs to monitor the oncogenic potential of Plk1 as well as study the effects of elevated Plk1 levels on Her2 or Kras driven breast cancer. The bulk of the initial work was the functional characterization of Plk1 overexpression *in vivo* in the mammary gland prior to and following tumor onset. The second part was focused on elucidating the molecular mechanisms leading to the observed phenotypes using *in vitro* culture systems. With this under consideration, the main objectives of this study can be broadly categorized as follows:

- Study the impact of Plk1 overexpression on tumorigenesis using inducible mouse models.
- Understand the molecular mechanisms and cellular processes that contribute to the observed phenotype.
- Explore the effect of Plk1 overexpression on mitosis and chromosome segregation.
- Elucidate the consequences of Plk1 induced polyploidy on tumor physiology.

Materials and Methods

In vivo Mouse Models

2.1 Generation of GEMMs

Mouse models utilized during the study were generated using KH2 ES cells provided by Konrad Hochedlinger and Rudolf Jaenisch (Beard et al, 2006). FLAG tagged human Plk1 cDNA cassette under the control of the tetracycline response element (tetO minimal promoter) was inserted at the ColA1 locus of the KH2 ES cells (Figure 2.1). These ES cells also contained the M2-rtTA gene inserted within the Rosa26 allele for the ubiquitous expression of the Plk1 transgene. The Malumbres laboratory (Cell Division and Cancer Group, CNIO) carried out the generation of ColA1-Plk1 animals. These animals were then crossed with MMTV-rtTA (Gunther et al, 2002), TetO-KrasG12D (Fisher et al, 2001), TetO-rat-Her2 (Moody et al, 2002), and H2B-GFP (Hadjantonakis & Papaioannou, 2004) animal models.

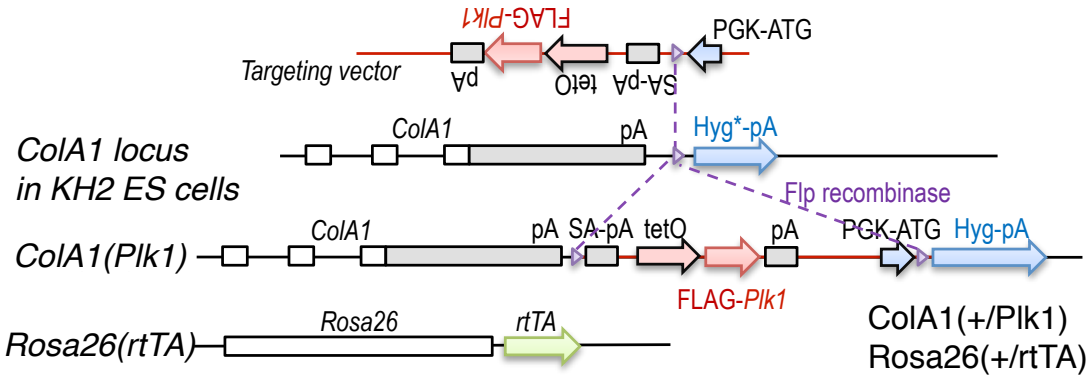

Figure 2.1: Schematic representation of alleles, cassette containing the human FLAG-Plk1 cDNA downstream of the tetO sequences is inserted in the ColA1 locus via FLP-FRT system, after homologous recombination in KH2 ES cells. Flippase (Flp) recombinase works by recognizing the Flp recombinase target (FRT) sequences flanking the region of interest. The ES cells are then selected using a hygromycin resistance cassette downstream of the insert. This allele ColA1-Plk1 is combined with the Rosa26-rtTA allele expressing the tetracycline transactivator.

2.2 Animal Husbandry and Monitoring of Disease

The mice for the study were housed in a specific pathogen free (SPF) environment with 12hr day-night cycles, average temperature of 21°C and humidity maintained at 55%. All breeding and experimental procedures were carried out at the DKFZ and EMBL Mouse Biology Unit. Procedures were in accordance with European Parliament directive (2010/63/EU) on protection of animals used for scientific purposes, current Italian legislation (Art. 9, 27. Jan 1992, no116) and the German Animal Welfare Act

(TierSchG, 1972) in addition to Animal Protection Laboratory Animal Regulations, 2013. *In vivo* induction of transgenes in adult female mice (8-10 weeks) was achieved using food pellets (625 mg/kg, Harlan-Teklad) containing doxycycline (stable tetracycline analogue). Experimental animals were monitored everyday by specialized technicians at the respective animal facilities. Progression of tumors was checked twice a week after tumor incidence and measurements were done using a vernier caliper. Human end point was determined when overall tumor volume reached or exceeded 1.5 cm, mice were sacrificed by cervical dislocation. All mice were maintained in a mixed FVB and C57BL/6J background.

2.3 Mouse Estrous Cycle

Pap smears were performed to check the estrous phase of the mouse. The vaginal lavage was done by carefully pipetting 50µl of 1x PBS into the vaginal canal of the mouse; the resuspended cells were spread onto a superfrost slide and allowed to dry. Crystal Violet (Sigma) staining was done for 1 min followed by 2-3 min of washing with water; the slides were then air dried and viewed under a microscope.

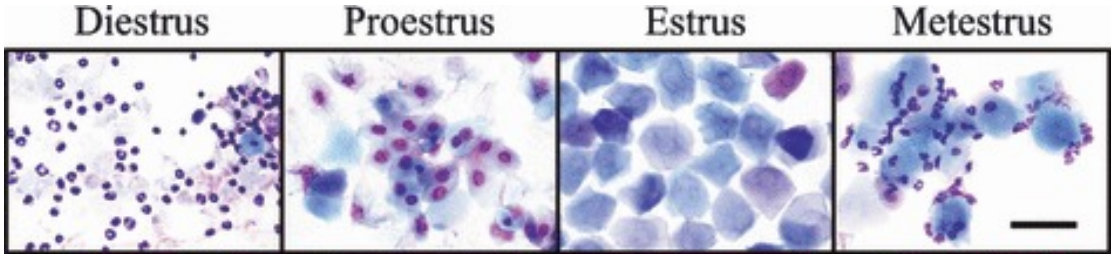

Figure 2.2: Cytological classification of pap smears as observed during different phases of the mouse estrous cycle (Aliagas *et al.* 2010).

2.4 Animal Necropsy

Necropsy tools and Styrofoam surface were disinfected with 70% ethanol prior to procedure. Mice were sacrificed by cervical dislocation and fixed in an upright position on the surface using pins. A vertical incision running across the body was made and the skin was pulled and pinned as displayed (Figure 2.3). All mammary glands were inspected prior to excision and any abnormal features were noted. The tissue samples were either collected in 10% neutral buffered formalin (Sigma) for histological processing or snap frozen with liquid nitrogen for DNA/RNA/protein work.

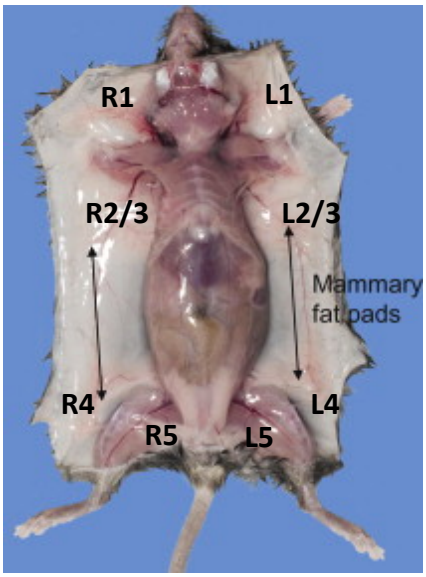

Figure 2.3: Necropsy of adult female mouse, labeling shows the position of all ten mammary glands of the animal. Image was adapted from Sue Knoblaugh, Julie Randolph-Habecker Steve Rath, in Comparative Anatomy and Histology, 2012.

2.5 Animal Surgery

For the surgical procedures, animals were maintained under constant anesthesia by isoflurane inhalation (1.5-3% in 0.8 L/min, Abbott) using a Non-Rebreathing anesthesia machine. Ophthalmic ointment was applied to the eyes of the mice to prevent drying. Surgical tools were autoclaved and then disinfected with 70% ethanol prior to procedures. The fur from the site of surgery was removed by local application of hair removal cream (Veet), following which the area was cleaned with 1x PBS. A small incision in the naked skin was made using a 10cm scissors and the mammary gland was carefully separated from the skin and subcutaneous layer using a forceps prior to excision with the scissors. The incision area was disinfected with betadine solution and it was closed using wound clips, animals were transferred to a clean cage placed under a heating pad to allow recovery after the procedure. The tissue sample was then collected for histology in 10% neutral buffered formalin or snap frozen in liquid nitrogen for RNA extraction.

2.6 Extraction of MEFs

Following the setting up of the breeding, the female mouse was monitored regularly for the vaginal plug and the exact date of which was noted. The mouse was sacrificed 12.5 – 13.5 days after the confirmation of vaginal plug and the embryos were collected in sterile 1x PBS. All further work was carried out in sterile conditions under a laminar flow cabinet. Embryos were carefully separated from the amniotic sac with a pair of tweezers, following which the head was removed for genotyping and the liver was separated from the rest of the body. This portion of the body was then digested overnight at 4°C with 500µl of 0.05% trypsin following which it was mechanically disassociated with a pipette and plated in a 150mm cell culture dish for further *in vitro* work.

2.7 Genotyping

Mice were weaned 3 weeks after birth and a small piece of the tail is removed for genotyping. DNA was extracted from mouse tail by incubation in 200µL 0.05M NaOH at 98ºC for 1.5h and subsequent neutralization with 20µL 1M Tris HCl ph7.5. For the genotyping of the MEFs, the heads of the embryos were digested with 400µL 0.05M NaOH at 98ºC for 1.5h followed by neutralization with 40µL 1M Tris HCl ph7.5. Each PCR reaction consisted of 1µl of extracted tail DNA and 20µl PCR mastermix which was composed of: Dream Taq Green Buffer (Thermo Scientific) 1X, 200 µM dNTPs, Taq Polimerase 1U/20µl, 0.25pmol/µl FW primer, 0.25 pmol/µl RW primer and dH_2O. The primers utilized for the different transgenes are listed below. The following PCR program was applied for all genes: 94°C for 2 min, 30 times [95°C for 30 s, 60°C for 30 s, 72°C for 30 s], and a final step at 72°C for 1 min.

Table: PCR Primers (Sigma)

Gene	Primer Name	Sequence
TetO-Kras	Kras4bfwd/DT12	GGGAATAAGTGTGATTTGCCT
	Kras4brev/rev mp1.2	GCCTGCGACGGCGGCATCTGC
ColA1-Plk1	Primer Coll frt A	GCACAGCATTGCGGACATGC
	Primer Coll frt B	CCCTCCATGTGTGACCAAGG
	Primer Coll frt C1	GCAGAAGCGCGGCCGTCTGG
Rosa26-rtTA	Common (HET)	AAAGTCGCTCTGAGTTGTTAT
	Wild type Reverse (WT)	GGAGCGGGAGAAATGGATATG
	Mutant Reverse (MT)	GCGAAG AGT TTG TCC TCAACC
MMTV-rtTA	CMV-rtTA F	GTGAAGTGGGTCCGCGTACAG
	CMV-rtTA R	GTACTCGTCAATTCCAAGGGCATCG
TetO-Neu	TAN-IRES 3528F	GACTCTCTCTCCTGCGAAGAATGG
	TAN-IRES 3914B	CCTCACATTGCCAAAAGACGG
H2B-GFP	H2B EGFP (F)	CAAGGGCGAGGAGCTGTT
	H2B EGFP (R)	AAGTCGTGCTGCTTCATGTG

2.8 Immunohistochemistry and Immunofluorescence of Tissue Sections

The samples obtained after necropsy (Section 2.4) were embedded in paraffin and sectioned at 3-5µm thickness using a rotary microtome (Leica) on to a superfrost slide. Standard protocol using xylene and ethanol was used for deparaffinization. Antigen retrieval step was carried out with 0,09% (v/v) unmasking solution (Vector) for 40min in a steamer, the slides were allowed to cool down to room temperature before washing with running water. After antigen retrieval, the tissue sections on the slides were encircled with a PAP pen (Sigma) and 3% H_2O_2 (Sigma) was applied on the sections to inactivate endogenous peroxidases. Species-specific VECTASTAIN

Elite ABC kits (Vector) were used as per manufacturer guidelines for blocking, secondary antibody staining and biotin-streptavidin binding. Primary antibody incubation durations varied depending on the specific antibody. Peroxidase reaction to detect primary antibody was carried out using DAB Peroxidase Substrate kit (Vector) and haematoxylin QS (Vector) was used for DNA counterstaining for the nuclei detection. Sections were dehydrated and mounted with DPX. Immunofluorescence was performed after deparaffinization of paraffin embedded tissue sections as described above. Permeabilization of tissue was then carried out using 1x PBS with 0.2% Triton X100 for 10min, blocking was achieved using 5% goat serum or donkey serum (Jackson Immuno) in PBS with 0.15 % Triton X100 for a duration of 1hr. Primary antibodies were diluted in blocking solution and incubated overnight at 4°C or 2hrs at room temperature. Following washes with 1xPBS, Alexa fluorophor labeled goat/donkey IgG (1:250, Invitrogen) secondary antibodies were incubated for 1hr at room temperature. DAPI (Life Technologies) was used for nuclear staining and mounted with Prolong Antifade mounting media. Imaging of immunohistochemistry sections was performed using Zen blue software (Zeiss) on a Zeiss Axioplan microscope. Slide scanning was carried out using the Zeiss Axioscan system or the TISSUEFAX (Tissuegnostics). Image analysis was done using Fiji (https://fiji.sc/) and Strataquest software (Tissuegnostics) for scanned sections. Primary antibodies used were against pH3 Ser10 (1:200, Cell Signaling, 9701), Pericentrin (1:3000, Abcam ab4448), γ-H2aX (1:500, Bethyl labs), p21 (1:50, Santa-Cruz SC-6246), PCNA (1:8000, Abcam ab18197), Plk1-phospho T210 (1:500, Abcam ab39068) and Plk1 (1:20, (Trakala et al, 2015)). TUNEL (In Situ Cell Death Detection Kit, TMR red, Roche, # 12156792910) was used for detecting cell death.

2.9 Interphase-FISH

For interphase-FISH, formalin fixed tissue was processed and sectioned as described in the previous section; similarly deparaffinization with xylene and rehydration with graded ethanol was carried out. Vysis Paraffin Pretreatment IV & Post-Hybridization Wash buffer kit was used as specified by the manufacturer. Probe mix was prepared with 3µl of labeled probe and 7µl Vysis LSI/WCP Hybridization buffer. The probe mix was spread on the tissue section and a 22x22mm coverslip (Prestige) was carefully placed on the section and sealed with Fixogum. Hybridization was performed using Thermobrite system (Abbott Molecular) with the following program: Denaturation 76ºC for 5 min, hybridization at 37ºC for 20-24 h. The pan-centromeric probes were made using pairs of BAC clones for each chromosome. Chr 16-RP23-290E4 & RP23-356A24 labeled with SpectrumOrange-dUTP (Vysis); and Chr 17-RP23-354J18 & RP23-202G20, labeled with SpectrumGreen-dUTP (Vysis); the BAC DNA were labeled by nick translation according to standard procedures. Imaging was done using Zen black software (Zeiss) on a Zeiss cell observer microscope. Signal for hybridization for

each probe was checked in a minimum of 60 interphase cells, image analysis was done using Fiji (https://fiji.sc/).

2.10 Whole Genome Sequencing (Low Coverage)

Snap frozen tissue was used for extraction of genomic DNA using DNeasy Blood & Tissue Kit (Qiagen) as per manufacturer guidelines. For Library preparation, the Beckman Biomek FX automated liquid handling system was utilized. SPRIworks HT chemistry (Beckman Coulter) was employed to provide total genomic DNA of 500ng as starting material. Quality control and library quantification was done with a Fragment Analyser (Advanced Analytics Technologies, Ames, USA). Illumina HiSeq 2500 platform (Illumina, San Diego, USA) was used for next generation sequencing. The DKFZ Genomics and Proteomics core facility handled library preparation and sequencing. For the analysis of the sequencing data, the reads were aligned to mm 10 build of mouse reference genome using BWA. Tumor coverage files were log2 normalized to genomic DNA obtained from normal mammary mouse tissue. Circular binary segmentation (R package, CBS) was applied and somatic copy number alterations (SCNA) were manually characterized as detailed: whole chromosome gains/losses are chromosome wide shifts in the segmentation of a chromosome whereas partial chromosome gains/losses entail losses/gains of at least 1/5 of the chromosome. Focal amplifications and deletions encompass events smaller than this. Gross chromosomal rearrangements were called when the number of copy number state switches on a chromosome exceeded a total of 10. The Korbel Laboratory (Genome Biology, EMBL Heidelberg) was responsible for analysis of all next generation sequencing data.

2.11 Real-Time Quantitative PCR

For RNA analysis, snap frozen tissue collected as described, was homogenized using a mortar and a pestle while using dry ice or liquid nitrogen to maintain temperature below –80ºC. RNA extraction was carried out following manufacturer's recommendations (RNeasy Mini Kit, Qiagen). QuantiTect Reverse Transcription Kit (Qiagen) was used for cDNA synthesis utilizing 400ng of RNA, measured using a Nano Drop 2000 (Thermo Scientific). Quantification using Real-time PCR was initiated using 12ng of cDNA with SYBR Green PCR Master Mix (2x) (Applied Biosystems) in LightCycler II® 480 (Roche). Relative gene expression was calculated as depicted: ΔCt = Ct (gene of interest) – Ct (housekeeping gene); ΔΔCt = ΔCt – ΔCt (reference sample); Relative Expression = 2^(–ΔΔCt). The list of primers is as follows:

Gene	Forward (5'-3')	Reverse (5'-3')
Actin B	GCTTCTTTGCAGCTCCTTCGT	ACCAGCCGCAGCGATATCG
Plk1	AACACGCCTCATCCTCTACAAT	AGGAGGGTGATCTTCTTCATCA
Her2	TGTACCTTGGGACCAGCTCT	GGAGCAGGGCCTGATGTGGGTT
Kras	AAGGACAAGGTGTACAGTTATGTGA	CTCCGTCTGCGACATCTTC
rtTA	CGCGTTATATGCACTCAGCG	TAAGAAGGCTGGCTCTGCAC

In vitro Culture Systems

2.12 MEF Culture and Live Imaging

Following the extraction protocol detailed in section 2.6, the MEFs were grown in Dulbecco's modified Eagle medium (DMEM; Gibco) supplemented with 2 mM glutamine, 1% penicillin/streptomycin and 10% tetracycline free foetal bovine serum (FBS; biowest). For live cell imaging, the MEFs were plated in a Poly-L-Lysine coated 8 well slide chambers (ibidi). Cultures were induced using 1µg/ml of doxycycline added to the culture media 6-8hrs prior to imaging. Treatment with Nocodazole (Sigma) and Paclitaxel (Sigma) was carried out by adding 1µM of the drug to the culture media 6hrs before imaging. Time-lapse imaging was performed for a duration of 12h using a Leica SP5 Confocal microscope: 2µm optical sectioning across 12µm stack, time-lapse of 5 min.

2.13 Chromosome Spreads

To perform chromosome spreads, MEFs were cultured to confluence in a standard 6 well culture plate and induced with 1µg/ml of doxycycline added to the culture media. Cells were arrested by treating with 1µM Nocodazole (Sigma) for 6-8h followed by 0.1µg/ml colcemid (Karyomax; ThermoFisher) for 2h. MEFs were collected by trypsinization; cytoplasm swelling was achieved by 75 mM KCl treatment for 15min and cells were fixed with fixative (3:1 methanol/acetic acid) for 20min. Fixed cells were splashed onto a superfrost slide placed in a humidified chamber to obtain chromosome spreads. The spreads were stained with Giemsa stain (Sigma) and imaging of samples was carried out using Zen black software (Zeiss) on a Zeiss cell observer microscope.

2.14 Focus Formation Assay

MEFs ($1x10^6$ cells) were plated in a standard 100mm culture dish and allowed to grow for 24h prior to transfection. To achieve transformation, cells were transfected with plasmids containing HRas-V12 and E1A using Calcium Phosphate transfection kit (Sigma) per manufacturer guidelines. MEFs were induced by treatment with 1µg/ml

of doxycycline added to the culture media. The cultures were monitored regularly to detect the formation of foci, 4 weeks after transfection the cells were fixed using 7:1 methanol/acetic acid and stained with 0.5% crystal violet solution. Following washes with distilled water, the dishes were allowed to dry and the number of foci was counted.

2.15 Immunofluorescence and Image Analysis

For immunofluorescence, MEFs were cultured on 19mm coverslips (VWR) in standard 12 well culture plates and induced with 1µg/ml of doxycycline added to the culture media. Cells were fixed using pre-warmed 4% PFA for 7min at 37°C or 1:1 methanol-acetone at -20°C followed by a wash with 1xPBS. Permeabilization of fixed cells was then carried out using PBS with 0.5% Triton X100 for 10min at 37°C, all subsequent washes were done using PBS with 0.15% Triton X100 at room temperature. Blocking was carried out with 10% goat serum or donkey serum (Jackson Immuno) in PBS with 0.15 % Triton X100 for a duration of 1hr. Primary antibodies were diluted in blocking solution and incubated overnight at 4°C or 2hrs at room temperature. After 3 washes for 5 min, secondary antibodies: Alexa fluorophore labeled goat/donkey IgG (1:250, Invitrogen) incubated for 1hr at room temperature. Coverslips were washed 3 times again before they were mounted on a superfrost slide using Prolong Antifade mounting media with DAPI. Primary antibodies against: Plk1 (1:2, (Trakala et al, 2015)), Plk1-phospho T210 (1:200, Abcam ab39068), Pericentrin (1:3000, Abcam ab4448), γ-Tubulin (1:1000, Sigma T6557), Sgo1 (1:100, S. Taylor, University of Manchester, England, UK), CREST-Texas Red conjugate (1:500, Antibody Inc), α tubulin (1:500, Sigma T6199) and α tubulin-FITC conjugate (1:500, Sigma F2168) were utilized. Leica TCS SP5 microscope with Leica LAS 4.5 software was used for imaging and image analysis was done using Fiji (https://fiji.sc/). For the quantification of mean fluorescence intensity, all images were converted to 8-bit grayscale following which cell borders were traced using the free hand tool in Fiji and mean pixel intensity for corresponding channel was calculated within the defined area.

2.16 Western Blotting

For protein detection by immunoblot, MEFs cultured to confluence in standard six well plates were collected using a cell scrapper. Cells were then lysed using RIPA lysis buffer (150mM NaCl, 50mM Tris pH 8, 1% Triton X100, 0.5% Sodium deoxycholate, 0.1% SDS) supplemented with PMSF (1:100) for 15 min on ice followed by centrifugation at 4°C, 14000rpm for 20 min. Quantification of protein was done using a spectrophotometer and Bradford reagent (Biorad). Proteins were first denatured by boiling at 100°C for 10 min and run on a 12% SDS poly-acrylamide gels (3.3ml dH2O, 4ml 30% acrylamide, 2.5ml 1.5M Tris pH 8.8, 100µl 10% ammonium

persulfate, 4µl TEMED) with stacking gel (1.45ml dH2O, 335ml 30% acrylamide, 250µl 1.5M Tris pH 6.8, 20µl 10% ammonium persulfate, 2µl TEMED) in running buffer (25mM Tris, 250mM glycine, 0.1% SDS) for several hours at 120V. Nitrocellulose membrane of appropriate size was activated with methanol and soaked in transfer buffer. Proteins were transferred onto the membrane using a TE 77 PWR semi-dry transfer unit (Amersham Biosciences) at 200mA for 1.5hrs following manufacturer guidelines. Membranes were washed with 1x TBS-T and blocking was done using 5% BSA in TBS-T for 1hr. Primary antibodies were diluted in blocking solution and incubated with the membrane, overnight at 4°C. For the detection of the protein, horseradish peroxidase-linked species-specific secondary antibodies: ECL anti-rabbit IgG (1:10000, NA934 Amersham) and ECL anti-mouse IgG (1:5000, NA931 Amersham) were used. The Blot was revealed by incubation with Amersham ECL™ Prime Western Blotting Detection Reagent for 3min, followed by imaging using LAS 400 Image Quant (GE) with an exposure time of 1-3min. Primary antibodies used for western blotting were: Actin (1:6000, A2066 Sigma), anti-FLAG (1:500, 2368s Cell Signaling) and anti-Plk1 (1:200, 4535s Cell Signaling).

2.17 Organoid Cultures

All 10 mammary glands of adult female mice were collected as described in section 2.4. The tissue was then digested overnight (37°C) with 20 mg/ml Liberase Blendzyme 2 (Roche, 11988425001) and 150 U/ml Collagenase type 3 (Worthington, no. CLS3) added to DMEM F-12 (Lonza) supplemented with 1% Hepes 1M (Gibco), 1% penicillin/streptomycin (Gibco). Tissue suspension was first mechanically disassociated with a pipette, followed by a single wash with sterile 1xPBS and further digestion with 0.25% trypsin at 37°C for 20 min. Trypsin was deactivated by washing with DMEM F-12 (Lonza) supplemented with 2 mM glutamine, 1% penicillin/streptomycin and 10% tetracycline free FBS (biowest). The cell suspension was then treated with DNAseI, after which they were resuspended in Mammary Epithelial Growth Media (MEGM; Lonza) and cultured overnight in BioCoat™ collagen coated 6well plates (Corning). This step was done to enrich the epithelial cell population in the culture. The cells were detached and collected by treatment with 0.25% trypsin at 37°C for 5min, the reaction was deactivated as described above and the cells were counted using an automated cell counter (Cellometer; Nexcelom Bioscience). A total of 12,000 cells were mixed with 90µl of 3D culture matrix (Matrigel; TEMA) and seeded as a single droplet onto Lab-Tek II chambered glass slides and allowed to polymerize for 20min at 37°C. The cells were cultured with MEGM for 6-8 days till acini formation (Figure 2.4) following which they are induced with 1mg/ml of doxycycline added to the culture media. Time-lapse imaging of organoid cultures was performed during 20h on an inverted spinning disk confocal (Perkin Elmer Ultraview-Vox): 0.3µm optical sectioning across 35µm stack, 5 frames/h and for a duration of 12h using a Leica SP8 Confocal microscope with a

resonant scanner: 0.9µm optical sectioning across 35µm stack, 12 frames/h. Image analysis was done using Fiji (https://fiji.sc/).

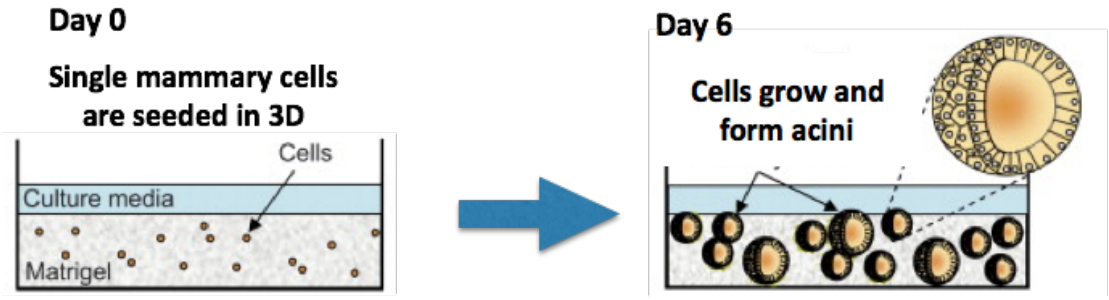

Figure 2.4: Seeding of single murine mammary epithelial cells in matrigel and development of organoids after 6-8 days in culture

2.18 Immunofluorescence of Organoid Cultures

For immunofluorescence of organoid cultures, it was first necessary to partially predigest the matrigel using 150 U/ml Collagenase type 3 (Worthington, no. CLS3) and 20 mg/ml Liberase Blendzyme 2 (Roche, no. 11988425001) added directly to the culture medium. Predigestion was carried out for the duration of 45min at 37°C, followed by washing thrice with 1xPBS before fixation using 4% PFA for 5min at RT. Cultures were then washed with 1x IF wash buffer (130 mM NaCl (Sigma), 7 mM Na2HPO4 (Sigma), 3.5 mM NaH2PO (Sigma), 7.7 mM NaN3 (Merck), 0.1 % BSA (Sigma), 0.2 % Triton-X (Sigma), 0.05 % Tween (Sigma), pH 7.4.), which was also used for all subsequent washes. Blocking was carried out for 1,5hrs using 10% goat serum (Jackson ImmunoResearch) and 1% AffiniPure F(ab')2 Fragment Goat Anti-Mouse IgG (Jackson ImmunoResearch) in 1x IF wash buffer. Primary antibodies were diluted in blocking solution and incubated overnight at 4°C. Cultures were washed 3 times for 30 min and incubated with Alexa fluorophor labeled goat/donkey IgG (1:800, Invitrogen) secondary antibodies. This was followed by 3 further washes for 30 min with 1x IF wash buffer and DAPI (1:2000). Cultures were then mounted with anti-fade agent Vectashield with Dapi (Vector laboratories). The primary antibodies utilized are: anti-Plk1-phospho T210 (1:200, Abcam ab39068) and anti-Pericentrin (1:3000, Abcam ab4448). Leica TCS SP5 microscope with Leica LAS 4.5 software was used for imaging and image analysis was done using Fiji (https://fiji.sc/).

2.19 Statistical analysis

GraphPad Prism 6 was utilized for all statistical testing. Control samples for in vivo experiments were obtained from animals containing the transgenes but kept on a normal diet or animals lacking MMTV-rtTA but placed under a doxycycline enriched diet. Non-induced cultures (–Dox) were considered as controls in vitro.

Results

The Effect of Plk1 Overexpression on Tumorigenesis

3.1 Plk1 does not function as an oncogene *in vivo*

The oncogenic potential of Plk1 has been widely debated over the past two decades. To finally put this debate to rest, our collaborators at the Malumbres laboratory (Cell Division and Cancer Group, CNIO) developed an inducible mouse model in which FLAG tagged human Plk1 is expressed under the Tet-inducible ubiquitous Rosa26 promoter (Section 2.1). When these mice were switched to a diet of food pellets with doxycycline (tetracycline analog) to induce transgene expression, they showed no significant difference in tumor free survival or percentage of spontaneous tumor incidence in comparison to the control group (Fig 3.1a, b). The mice lacking the Plk1 transgene (+/+);(+/rtTA) served as controls and the animals heterozygous for Plk1 and Rosa26-rtTA (+/Plk1)(+/rtTA) formed the experimental group. These results suggested that Plk1 when overexpressed *in vivo* lacked any oncogenic potential. Guillermo de Cárcer from the Malumbres laboratory carried out the initial characterization of the Plk1 mouse model.

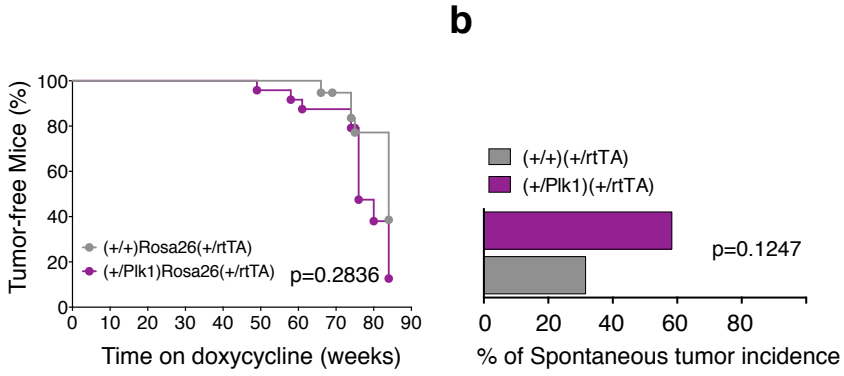

Figure 3.1: a) Tumor-free survival of (+/+) ;(+/rtTA) and (+/Plk1)(+/rtTA) mice fed with Dox since birth during 85 weeks. (+/+)(+/rtTA), 19 mice; (+/Plk1)(+/rtTA), 24 mice. p=0.2836; Log-rank (Mantel-Cox) Test. b) Percentage of mice with spontaneous tumors. (+/+)(+/rtTA), 19 mice; (+/Plk1)(+/rtTA), 24 mice. p=0.1247; (Data courtesy of Malumbres laboratory, CNIO, Spain).

3.2 Overexpression of Plk1 delays mammary tumor initiation in Kras and or Her2 driven breast cancer models.

For studying the effect of elevated levels of Plk1 during mammary tumorigenesis, we generated new mouse models by crossing mice containing the tetracycline inducible Plk1 with mice of Kras/Her2 oncogenic background, in which the mammary specific MMTV-rtTA promoter controls the gene expression (Section 2.1). The progenies of these crosses were used for this study. Female transgenic mice above the age of 8

weeks were put on a doxycycline diet to switch-on the expression of the transgenes present.

Plk1 overexpression on its own did not display any oncogenic potential and behaved similar to the control cohort; these findings were in line with the data from the Malumbres laboratory for the ubiquitous overexpression of Plk1, described earlier. In combination with the oncogenes $Kras^{G12D}$ or Her2, it was observed that Plk1 played a tumor suppressive role by significantly delaying tumor initiation. The overexpression of the oncogene $Kras^{G12D}$ yielded mammary tumors in mice at around 172 days, whereas $Kras^{G12D}$/Plk1 animals took significantly longer to develop tumors and tumor development was completely suppressed in 90% of the colony (Figure 3.2a). In the Her2 mice the first palpable tumors were observed at around 112 days after doxycycline induction, in comparison Her2/Plk1 animals developed tumors much later around 349 days following induction and in addition Plk1 overexpression also completely prevented tumor development in 52% of the total colony (Figure 3.2b). It must be noted that mice have 10 mammary glands; each of them can potentially develop tumors, however elevated levels of Plk1 also reduced number of mammary glands that underwent transformation (Figure 3.2c).

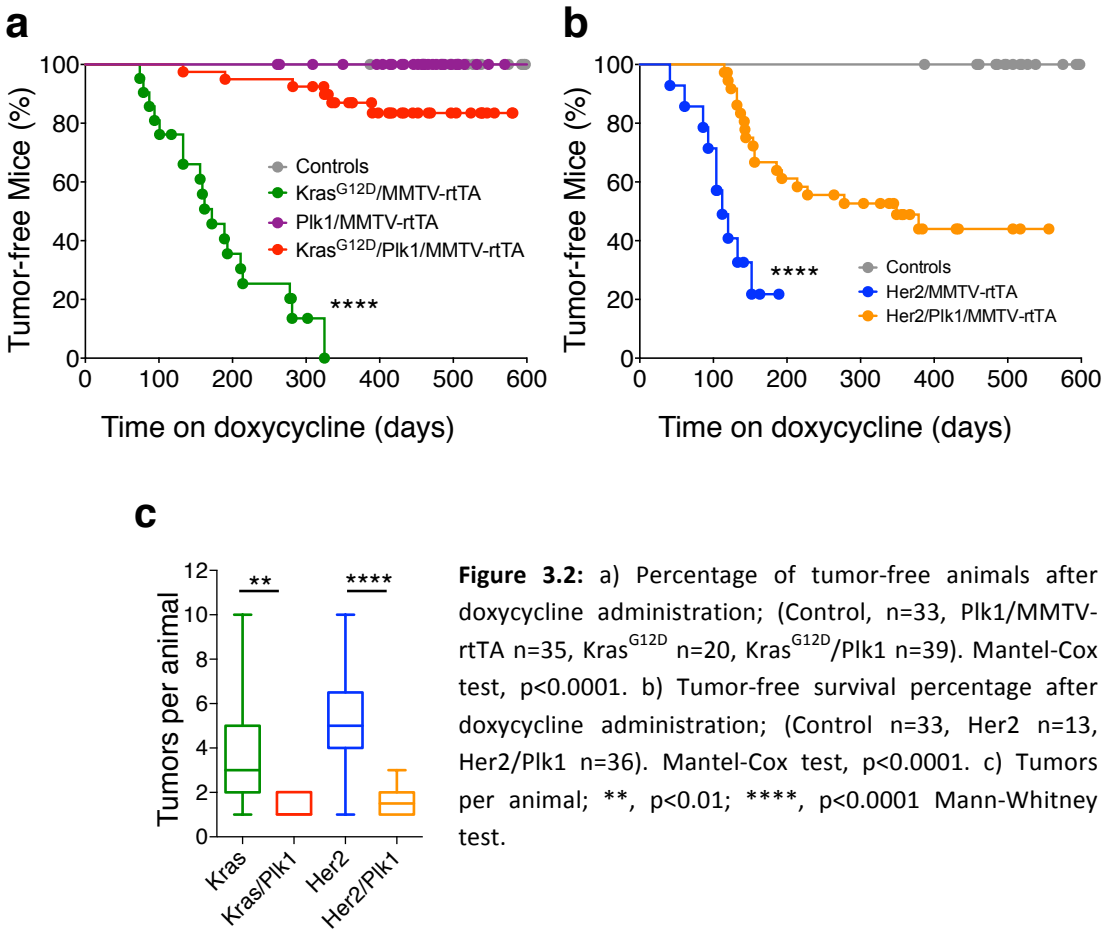

Figure 3.2: a) Percentage of tumor-free animals after doxycycline administration; (Control, n=33, Plk1/MMTV-rtTA n=35, $Kras^{G12D}$ n=20, $Kras^{G12D}$/Plk1 n=39). Mantel-Cox test, p<0.0001. b) Tumor-free survival percentage after doxycycline administration; (Control n=33, Her2 n=13, Her2/Plk1 n=36). Mantel-Cox test, p<0.0001. c) Tumors per animal; **, p<0.01; ****, p<0.0001 Mann-Whitney test.

3.3 Consequence of Plk1 overexpression on tumor progression

Histological analysis of the mammary tumors revealed that those tumors with elevated Plk1 levels clearly displayed an increase in the frequency of polyploidy, denoted by cells with increased nuclear volume. Figure 3.3 clearly depicts that there is a significantly higher percentage of these cells with increased nuclear volume in tumors with Plk1 overexpression when compared to normal mammary gland control as well as single oncogene tumors. Increased nuclear volume is a phenotype usually associated with higher total genomic content resulting from polyploidy. Genome doubling events leading to polyploidy have been proposed to be early stage events leading to tumor initiation (Kirkland, 1966). The timing and exact mechanism by which elevated Plk1 results in tetraploidization will be a topic of discussion later.

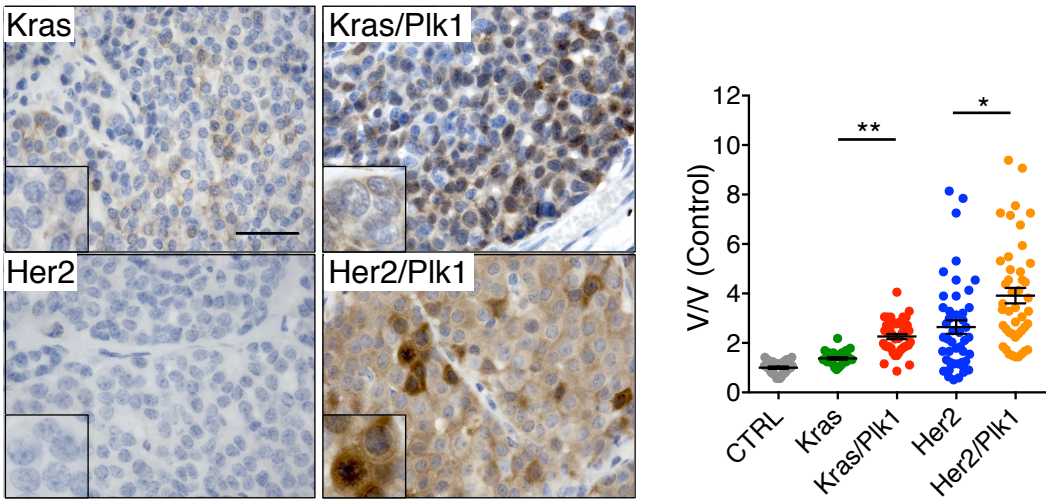

Figure 3.3: Immunohistochemistry against Plk1 in paraffin sections of mammary tumors. Scale bar 20µm. Graph depicts quantification of nuclear volume of tumors relative to control cells at 100days on doxycycline (CTRL: n=30; Kras: n=30; Kras/Plk1: n=40; Her2: n=46; Her2/Plk1: n=45); points represent single nuclear measurements; Kruskal-Wallis test, Dunn's multiple comparisons test. *$p < 0.05$, **$p < 0.01$. Number of animals: (CTRL: 3; Kras: 4; Kras/Plk1: 4; Her2: 5; Her2/Plk1: 5).

3.4 Genome doubling caused by elevated Plk1 promotes the tolerance of aneuploidy

Polyploid cells are a common occurrence in several solid tumors and recent studies support the hypothesis that these cells resulting from genome-doubling events are an intermediary step to aneuploidy in tumors (Davoli, de Lange and Lange, 2011). To validate if this holds true in our genetically engineered mouse models, we utilized I-FISH to verify the frequency of aneuploidy in the different tumor models described earlier. Results indicated that the tumors that harbored a higher percentage of polyploid cells also showed the highest frequency of aneuploidy (Figure 3.4). In this case Plk1 overexpression in the tumors correlates with increased tolerance of aneuploidy. This is in line with recent findings demonstrating that whole genome

doubling promotes chromosomal instability which causes aneuploidy (Dewhurst *et al.*, 2014). Chromosomes 16 and 17 were counted and cells were considered aneuploid if they housed more than the usual diploid (2n) chromosome count for either. Tetraploid cells were identified as those that harbored 4n or more chromosomes.

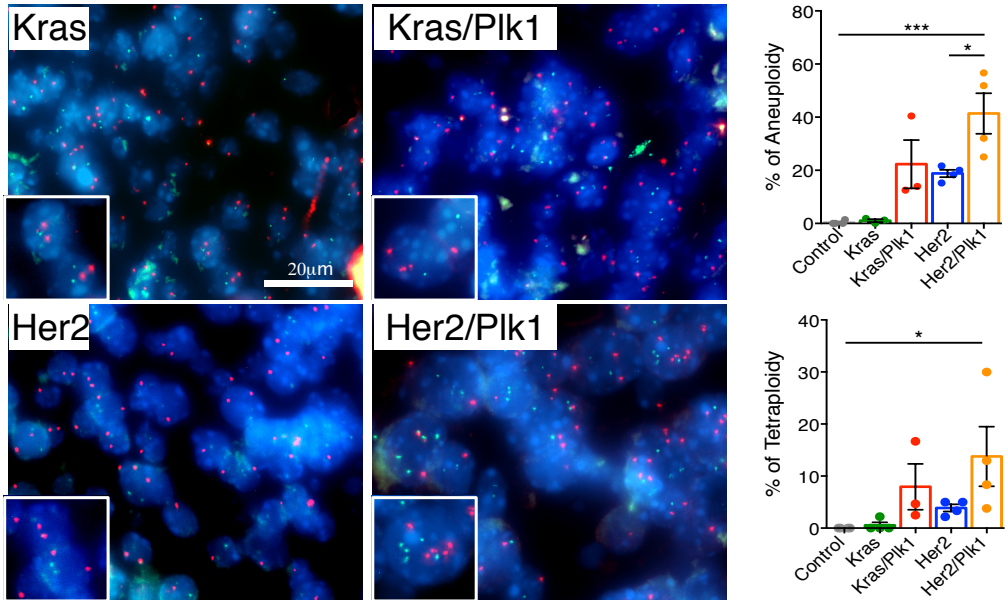

Figure 3.4: Interphase-Fluorescent in situ hybridization (I-FISH) on paraffin sections of mammary tumors using two centromeric probes against chromosomes 16 and 17. Histograms display quantification of the frequency of aneuploidy (top) and tetraploidy (bottom) in samples from the indicated genotypes (Control, n=4; Kras, n=4; Kras/Plk1, n=3; Her2, n=4; Her2/Plk1, n=4 mice). *, $p<0.05$; ***, $p<0.001$; One-way ANOVA.

The results from the I-FISH were supplemented by the data obtained from whole genome sequencing (WGS) of the Her2 and Her2/Plk1 tumors, the Kras/Plk1 tumors were not sequenced due to lack of material. This method of low coverage WGS can be used to detect any chromosomal aberrations that are present in a majority (60% or more) of the cells from a tumor. WGS is limited in terms of histological context and single cell level resolution demonstrated by I-FISH, however it makes up for that by contributing precise structural resolution for the entire genome. A total of 10 Her2 tumors and 9 Her2/Plk1 tumors were sequenced and somatic copy number alterations (SCNAs) per tumor were analyzed. The SCNAs were divided into separate categories as follows: whole chromosome gain (WCG) and loss (WCL), partial chromosome gain (PCG) and loss (PCG), focal amplification (AMP), focal deletion (DEL) and gross chromosomal rearrangements (GCR) (Figure 3.5a). Overall, the Her2 tumors displayed an average of 2.3 SCNA compared to the Her2/Plk1 tumors with an average of 4 SCNAs per tumor (Figure 3.5b). The Her2/Plk1 tumors presented with AMP, frequent DEL and GCR, which were completely absent in Her2 tumors (Figure

3.5a). Analysis of the sequencing data was carried out by Christopher Buccitelli, Korbel Group, EMBL Heidelberg.

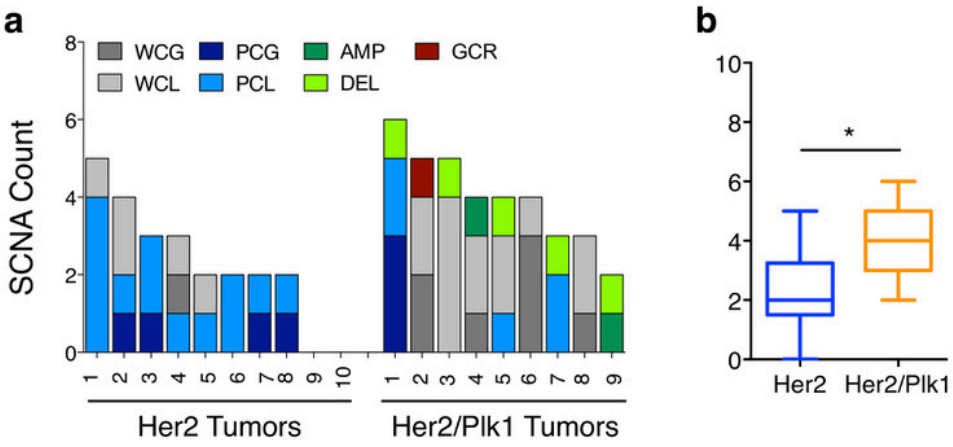

Figure 3.5: a) SCNAs in 10 Her2 and 9 Her2/Plk1 tumors. SCNAs categorized as WCG, WCL, PCG, PCL, AMP, DEL and GCR. b) Average SCNAs in primary tumors (Her2: n=10; Her2/Plk1: n=9); Mann-Whitney test. *, $p < 0.01$. Data analysis performed by Christopher Buccitelli, Korbel Group, EMBL Heidelberg.

3.5 Tumors over expressing Plk1 proliferate less and have more G1 arrested cells

A common consequence of polyploidy is the activation of p21 through p53 dependent mechanism resulting in cell cycle arrest (Ganem and Pellman, 2007). In agreement with the literature, immunohistochemistry staining of p21 revealed that the tumors with elevated Plk1, which possessed higher percentage of polyploid cells, also displayed more p21 positive cells (Figure 3.6a). The percentage of cells that were still proliferating in these tumors was determined by PCNA staining and as expected, the results were reversed, the tumors with elevated Plk1 displayed an overall lower proliferation than the single oncogene tumors (Figure 3.6b). The tumors overexpressing Plk1 had lower proliferation rates and higher percentage of G1 arrested cells as indicated by the p21 staining.

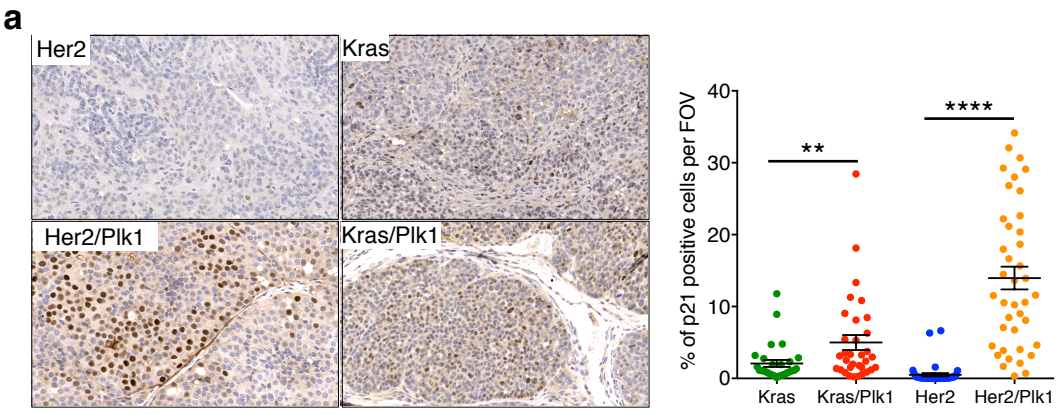

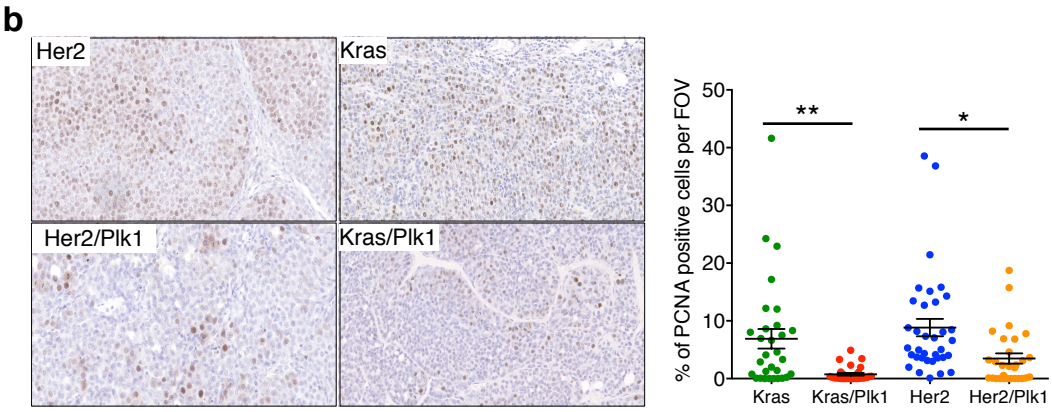

Figure 3.6: a) Immunohistochemistry against p21 in paraffin sections of mammary tumors and quantification of percentage of positive cells per field of view (FOV per genotype - Kras: n=30; Kras/Plk1: n=33; Her2: n=40; Her2/Plk1: n=45); points represent percentage of positive cells per FOV; Ordinary one-way ANOVA. **p < 0.01, ****p < 0.0001. Number of animals: (Kras: 3; Kras/Plk1: 3; Her2: 4; Her2/Plk1: 4). b) Immunohistochemistry against PCNA in paraffin sections of mammary tumors and quantification of percentage of positive cells per field of view (FOV per genotype - Kras: n=30; Kras/Plk1: n=30; Her2: n=36; Her2/Plk1: n=29); points represent percentage of positive cells per FOV; Ordinary one-way ANOVA. **p < 0.01, *p < 0.05. Number of animals: (Kras: 3; Kras/Plk1: 3; Her2: 3; Her2/Plk1: 3).

Monitoring early stage events prior to tumor initiation

3.6 Plk1 overexpression in mammary glands prior to tumor initiation

Prior to studying the effects of Plk1 over expression in tumors from these mouse models, it was initially necessary to confirm the levels of expression of the transgene, as well as validate if the model depicted the human scenario as accurately as possible. To achieve these goals, we performed immunohistochemistry against Plk1 in mammary glands obtained from the models described in section 3.2. The mammary glands were collected at 4 days and 100 days after the administration of doxycycline, to study expression levels as well as gradual changes in morphology of the organ prior to transformation. All mammary glands were surgically removed at the pro-estrous phase to control for changes induced by hormonal fluctuations as described (Section 2.3, 2.4).

Observations revealed that, Plk1 expression was stable over time in the relevant transgenic models and it was absent in the age-matched controls. We also confirmed that the tumors from these mice continued to over express Plk1 and the expression was not completely lost because of malignant transformation, despite the strong tumor suppressive effects demonstrated in section 3.2. In addition, we observed that, while mammary glands from the Kras and Her2 animals showed signs of neoplastic growth at 100days, the animals that had Plk1 over expression had relatively normal mammary gland morphology (Figure 3.7).

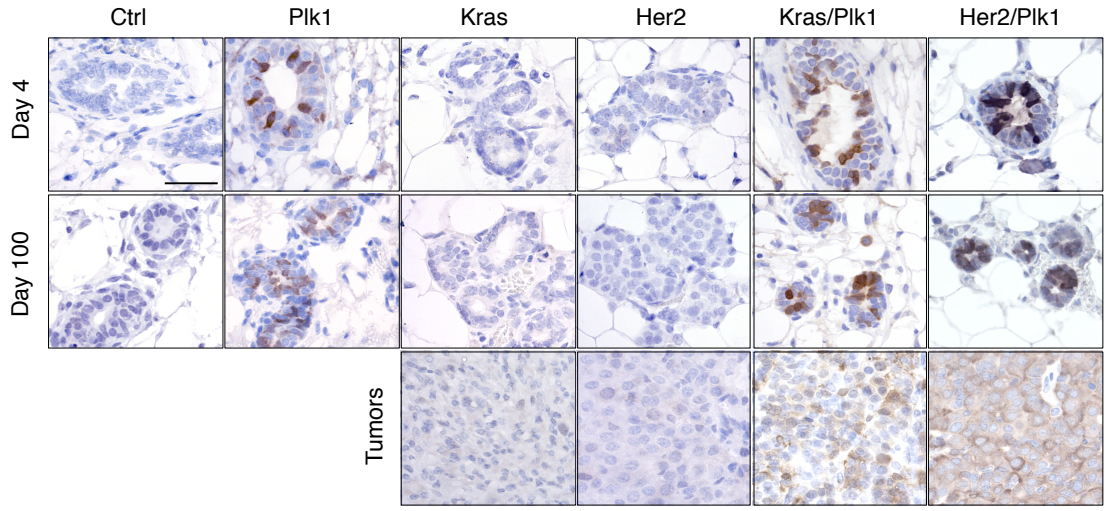

Figure 3.7: Immunohistochemistry against Plk1 in paraffin sections of tumors plus mammary glands 4 days and 100 days on doxycycline. Scale bar 50µm.

Analysis of the levels of the transgenic Plk1 using RT-qPCR (Figure 3.8a) showed that the average level of gene expression in the different models did not exceed the range of Plk1 expression observed in human breast cancer cell lines as depicted in Figure 3.8b.

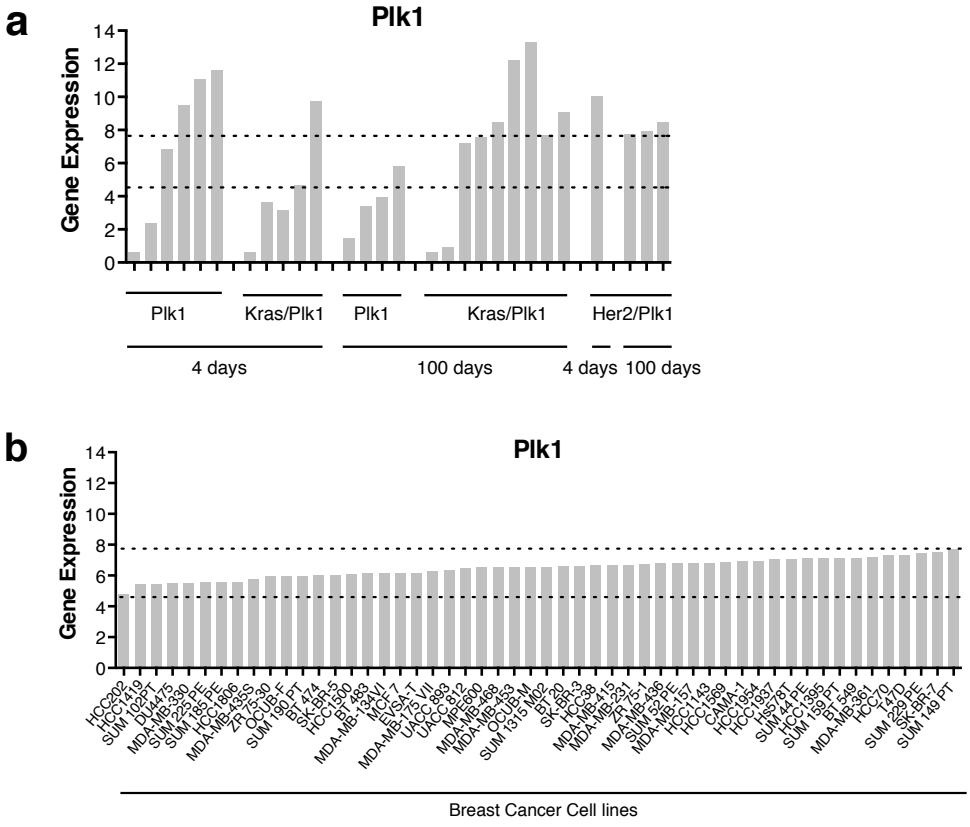

Figure 3.8: a) RT-qPCR showing relative expression of transgenic Plk1 in mammary glands 4 days and 100 days on doxycycline. b) Gene expression of Plk1 in 51 different breast cancer cell lines (Neve *et al.*, 2009).

3.7 Increase in genomic content and centrosome number as a consequence of Plk1 overexpression occurs at a very early stage

As discussed previously, elevated levels of Plk1 resulted in a higher percentage of polyploidy in the mammary tumors. To better determine the timing of the genome-doubling event, we performed histological analysis of mammary glands prior to tumor development and measured the nuclear volume of cells over expressing Plk1, per mammary acini. Surprisingly there was an increase in overall nuclear volume as early as 4 days following induction of Plk1 overexpression (Figure 3.9a), indicating the effect of Plk1 on genome doubling of cells was an early event. The increase in percentage of polyploidy was also accompanied with a significantly higher percentage of cells per mammary acini with 3 or more centrosomes (Figure 3.9b). Supernumerary centrosomes are a common consequence of tetraploidization (Meraldi, Honda and Nigg, 2002).

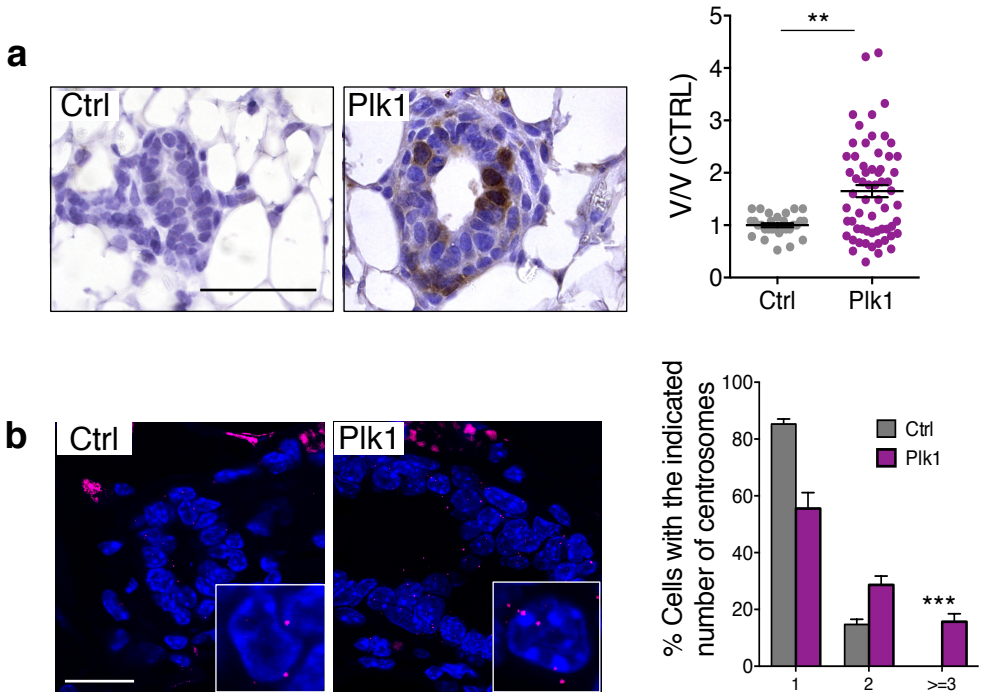

Figure 3.9: a) Immunohistochemistry against Plk1 in paraffin sections of mammary glands and quantification of Nuclear volume relative to control cells at 4days on doxycycline (Ctrl: n=30; Plk1: n=62) **p < 0.01; Mann-Whitney Test. Points represent single nuclear measurements. Number of animals: (Ctrl: 3; Plk1: 6); Scale bar 20µm. b) Immunofluorescence against pericentrin in paraffin sections of mammary glands and quantification of percentage of cells per acini with 1,2 or 3 centrosomes at 4days on doxycycline (Ctrl: n=170; Plk1: n=352) ***p < 0.001; Mann-Whitney Test. Number of animals: (Ctrl: 3; Plk1: 3); Scale bar 20µm.

3.8 Effect of Plk1 on proliferation and cell death

Upon confirming that Plk1 overexpression led to tetraploidization at the 4-day time point, it was essential to determine if this inadvertently influenced proliferation or

cell death. Immunohistochemistry against Phospho-Histone3, which is commonly used as a marker of proliferation and immunofluorescence for TUNEL to detect the presence of apoptotic cells was performed. Although, the mammary glands with Plk1 over expression showed an overall increase in the percentage of pH3 positive cells in comparison to controls, there was no significant difference when compared to mammary glands from the Kras model. The results for the quantification of the percentage of TUNEL positive cells revealed a similar picture; elevated levels of Plk1 significantly increased apoptosis with respect to the control mammary glands however not when compared to single oncogene control. Surprisingly the mammary glands from Kras/Plk1 animals also showed an increase in percentage of pH3 and TUNEL positive cells, although this effect was not compounded (Figure 3.10a, b).

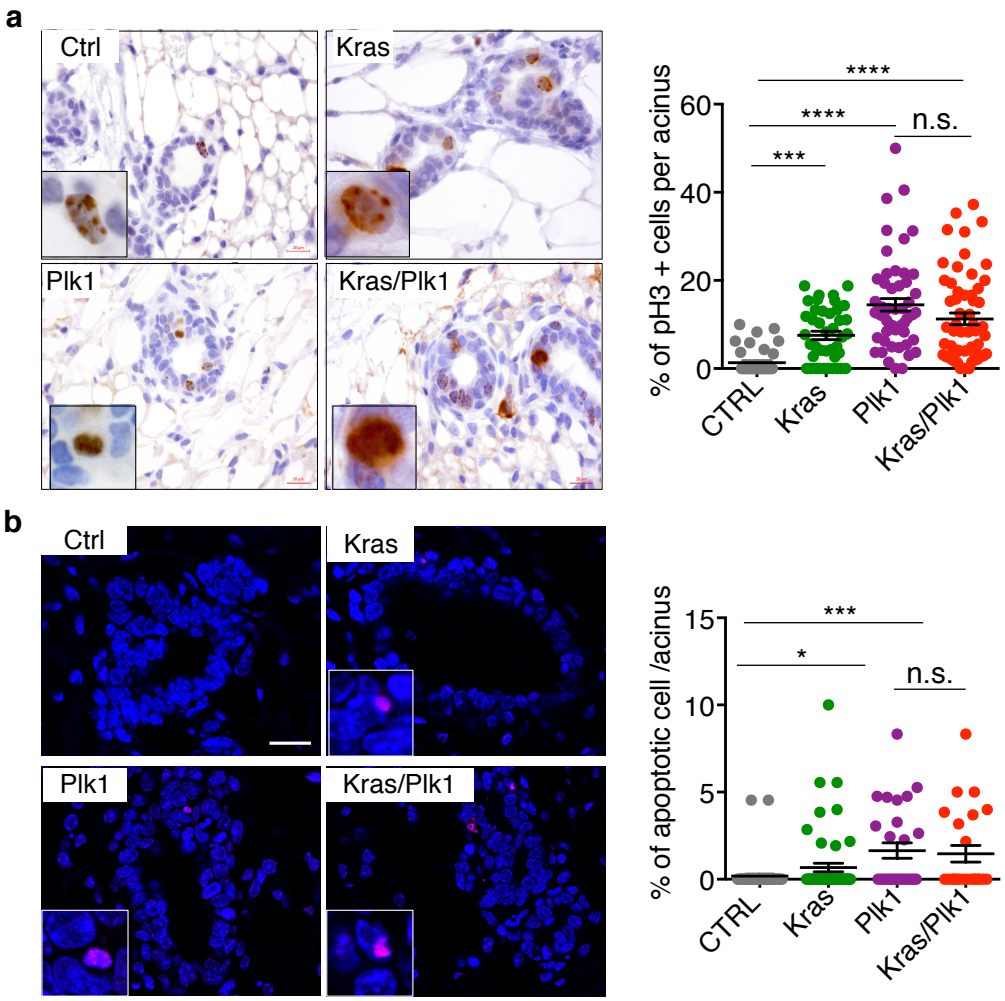

Figure 3.10: a) Immunohistochemistry against phospho-H3 in paraffin sections of mammary glands 4 days on doxycycline. The histogram shows the percentage of pH3 positive cells per acinus (Ctrl: n=42 acini; Kras: n=42 acini; Plk1: n=53 acini; Kras/Plk1: n=58 acini). Kruskal-Wallis test, Dunn's multiple comparisons test. ***p < 0.001, ****p < 0.0001, ****p < 0.0001. Each point represents single acini and total quantification includes minimum 6 animals per genotype. b) Immunofluorescence using TUNEL kit in paraffin sections of mammary glands 4 days on doxycycline. The plot shows the quantification of percentage of TUNEL positive cells per acinus (Ctrl: n=51 acini; Kras: n=56 acini; Plk1: n=28 acini; Kras/Plk1: n=24 acini) Kruskal-Wallis test, Dunn's multiple comparisons test. ***p < 0.001,

*p < 0.05. Each point represents single acini and total quantification includes minimum 4 animals per genotype.

Thus, it was possible to conclude Plk1 overexpression influences proliferation and cell death in the mammary gland, however this is not significantly different from the effects caused by oncogene induction.

Mouse Embryonic Fibroblasts (MEFs)

3.9 Plk1 over expression leads to reduced proliferation and increased frequency of mitotic aberrations

Earliest studies charactering the function of Plk1 showed that in the absence of this kinase, chromosomes failed to orient in a proper bi-polar spindle, instead forming mono polar spindles (Sunkel and Glover, 1988). It was also observed that Plk1 had prominent roles in controlling the timing of mitotic entry as well as abscission during cytokinesis. Considering the several functions of Plk1 during cell division and furthermore to explain the phenotype of polyploidy observed *in vivo*, we decided to investigate the effect over expressing Plk1 has on mitotic cells using MEFs derived from the Rosa26 ubiquitous mouse model described previously (Section 3.1). Unless specifically mentioned all experiments were carried out with heterozygous (+/Plk1)(+/rtTA) MEFs. The induction of the Plk1 transgene was confirmed by performing western blot for FLAG tagged Plk1 after treatment with doxycycline for 12h (Figure 3.11a). These initial observations were essential to confirm Plk1 overexpression in MEFs before proceeding to more elaborate studies. MEFs provide an extremely versatile system to answer mechanistic questions that can help the validation of *in vivo* phenotypes.

Overexpression of Plk1 in primary MEFs led to reduced proliferation in these cultures, monitored for 5 days post induction (Figure 3.11b). Furthermore, immunofluorescence of MEFs after 24h of induction with doxycycline revealed that a significant number of cells with elevated Plk1 displayed an array of mitotic aberrancies as represented below (Figure 3.11c). The mitotic errors were categorized as the following: monopolar spindles, multipolar spindles, lagging chromosomes and chromosome bridges.

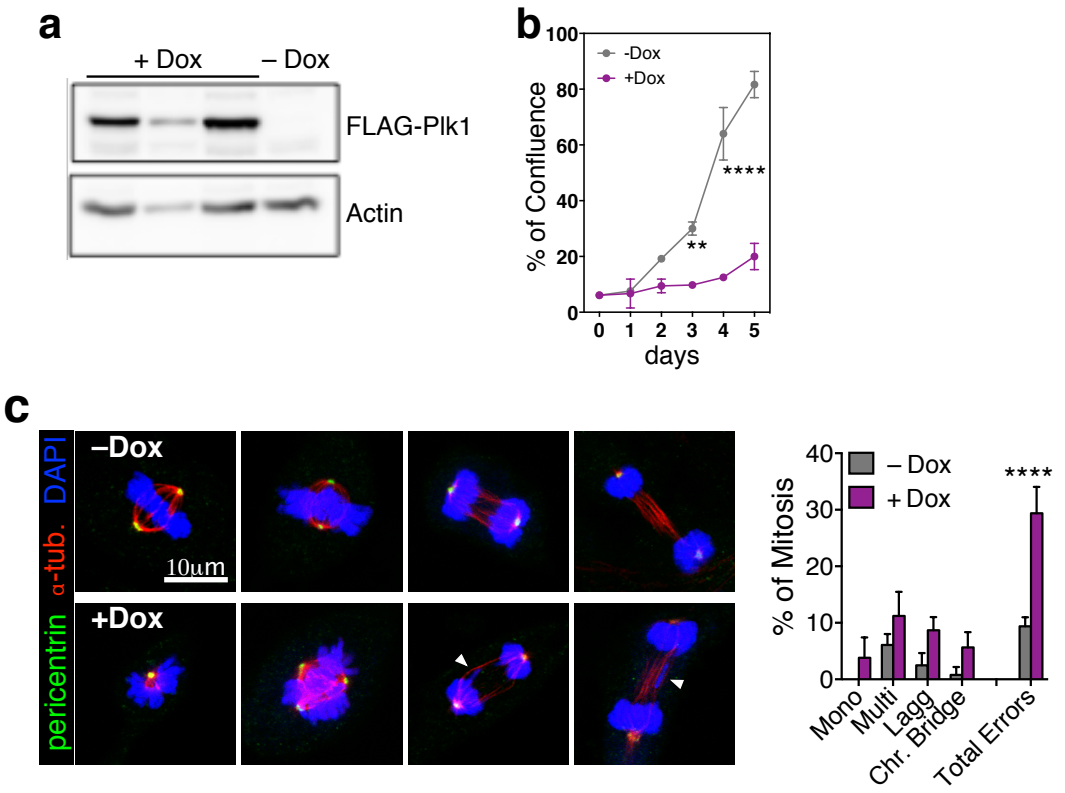

Figure 3.11: a) FLAG-Plk1 western blot of protein extracts obtained from Plk1/Rosa26-rtTA MEFs (ON Dox: n=3 replicates; OFF Dox: n=1 replicate). b) Quantification of confluence in cultures in the absence (–Dox) or presence (+Dox) of Doxycycline for 5 days. **, p<0.001 ****, p<0.0001; Two-way ANOVA. c) Immunofluorescence against α-Tubulin and pericentrin in primary MEFs after 24h on doxycycline induction followed by quantification of the percentage of mitotic aberrancies (–Dox: n=149 mitotic cells; +Dox: n=166 mitotic cells). ****, p<0.0001; 2way ANOVA.

3.10 Plk1 suppresses oncogenic transformation *in vitro*

The results from section 3.2 indicated that Plk1 overexpression strongly suppressed $Kras^{G12D}$ and Her2 driven mammary tumorigenesis. It was imperative to determine if this was a tissue or oncogene specific effect, for this we analyzed if Plk1 overexpression could suppress *in vitro* transformation of primary MEFs by oncogenic HrasV12 and E1A. Focus formation assays performed using Plk1/Rosa26-rtTA MEFs transfected with oncogenic HrasV12 + E1A revealed that when Plk1 overexpression was induced by doxycycline there was a drastic reduction in the number of transformed foci (Figure 3.12). These results suggested that Plk1 overexpression could suppress oncogenic transformation *in vitro*.

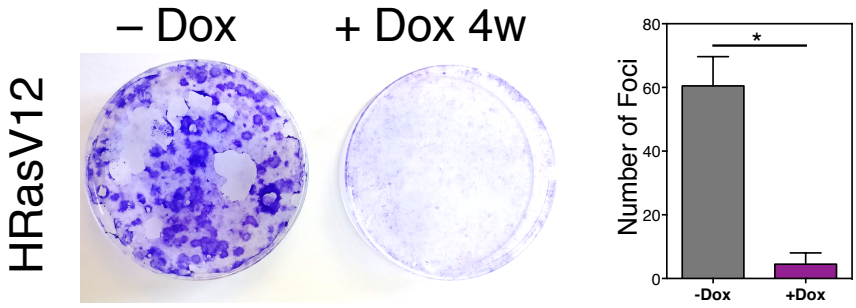

Figure 3.12: Focus formation assays of Plk1/Rosa26-rtTA MEFs transfected with oncogenic HrasV12 + E1A in the absence (–Dox) or presence (+Dox) of Doxycycline for 4 weeks. The number of foci is indicated in the histogram. *, $p<0.05$ (n=2 replicates); Unpaired t test.

3.11 Plk1 increases the percentage of polyploidy

It was essential to validate if the MEFs recapitulated the *in vivo* phenotype accurately. To check if the MEFs over expressing Plk1 were polyploid, flow cytometry based analysis was performed by our collaborators at the Malumbres laboratory. Total DNA content per cell after treatment with doxycycline for 24h and 48h was determined. In line with the *in vivo* data, the Plk1/Rosa26-rtTA MEFs showed a steady increase in the number of genome-doubled cells with increased time of doxycycline treatment. This data further supports that Plk1 induces polyploidy by a previously unexplored mechanism.

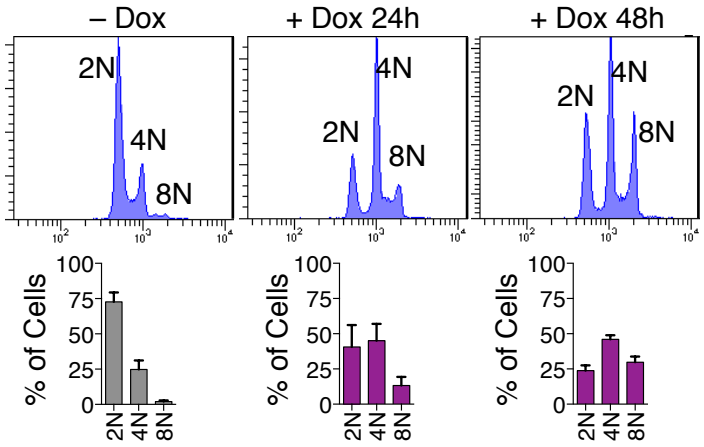

Figure 3.13: DNA content of Plk1/Rosa26-rtTA MEFs (homozygous for Plk1 and Rosa26-rtTA), untreated or treated with Dox for 24h and 48h respectively. The percentage of 2N, 4N or 8N cells is indicated in the histograms (Data courtesy of Malumbres laboratory, CNIO, Spain).

3.12 Elucidating the mechanism of Plk1 induced polyploidy

The cumulative results showed an increase in polyploidy and mitotic aberrations, indicating possible defects in mitotic progression. This hypothesis was verified by performing time-lapse imaging of Plk1/Rosa26-rtTA/H2B-GFP MEFs after treatment with doxycycline for the duration of 8h. Images were captured every 5 minutes with

the total session lasting 12h. Fate of a mitotic cell was classified based on observed phenotypes as: regular mitosis, cytokinesis failure, no segregation and mitotic regression.

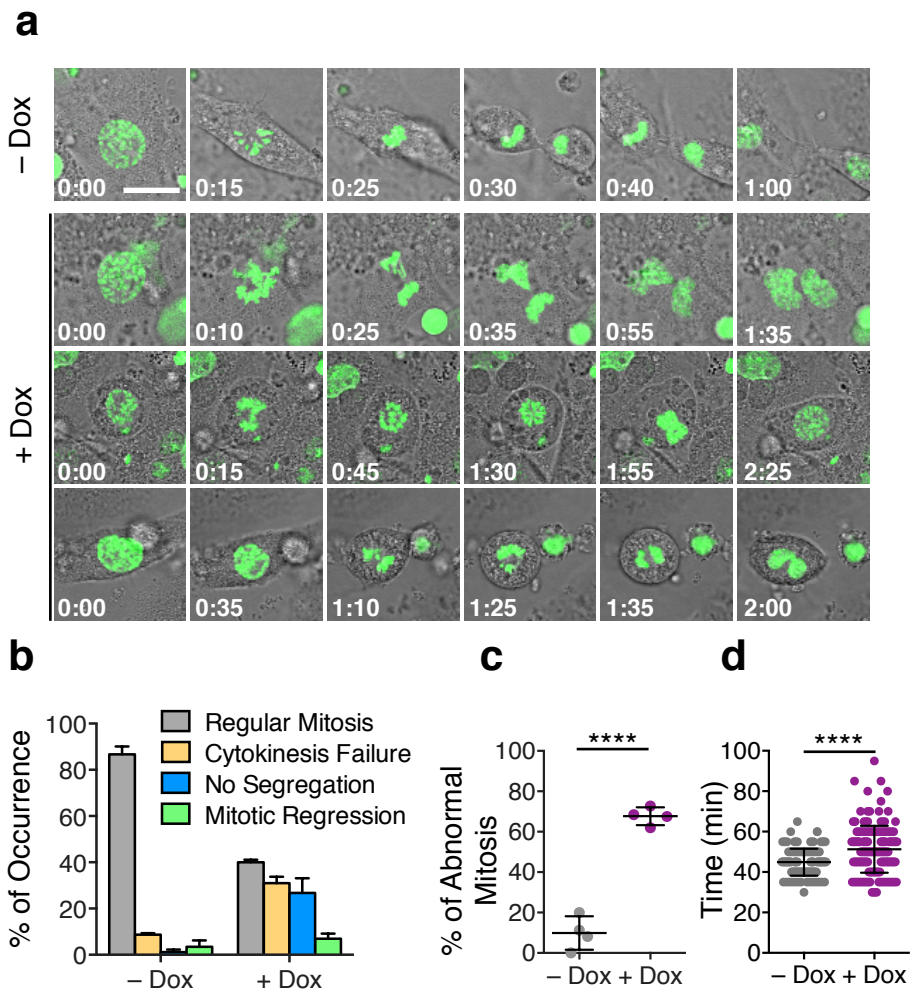

Figure 3.14: a) Time-lapse microscopy of Plk1/Rosa26-rtTA MEFs off Dox (upper panel) and after 8h on doxycycline (lower panels), indicating mitotic cells; H2B-GFP (green), classified based on the three major phenotypes resulting in a tetraploid progeny in the case of Plk1 overexpression. Scale bar 20µm. b) Percentage of occurrence of each major phenotype in –Dox (n=141) and +Dox (n=164) MEFs. c) Percentage of mitotic errors per MEF (–Dox: 141 cells; +Dox: 164 cells); points represent individual MEF line. ****, p<0.0001, Unpaired T-test. d) Duration of mitosis in the MEF cultures (–Dox: 141 cells; +Dox: 164 cells). ****, p<0.0001, Unpaired T-test.

Results indicated a significant percentage of cells (26.7% versus 1.1% in control cells) exited from mitosis prior to anaphase, without chromosome segregation. In addition, 38% of Plk1-overexpressing cells displayed abnormal cytokinesis resulting in binucleated cells or underwent mitotic regression thereby generating tetraploid cells with a single nucleus (Figure 3.14a, b)

Timing in mitosis was calculated from the point of nuclear envelope breakdown (NEBD) till attachment; it was also interesting to note that the MEFs over expressing Plk1 displayed a slight increase in mitotic timing (Figure 3.14d). This experiment was

clearly able to demonstrate that Plk1 overexpression resulted in genome doubling by mainly two independent mechanisms, either due to complete lack of segregation or failure at cytokinesis.

3.13 Activation and localization of Plk1 during different mitotic phases

Both the functions and the localization of Plk1 during different phases of mitosis have been well characterized (De Cárcer, Manning and Malumbres, 2011). Owing to the results from earlier it was a fair assumption that the elevated levels of induced Plk1 resulted in increased activity of the kinase during mitosis. We verified this by staining doxycycline treated MEFs with an antibody that recognizes phosphorylation on Thr210 at the Plk1 T-activation loop.

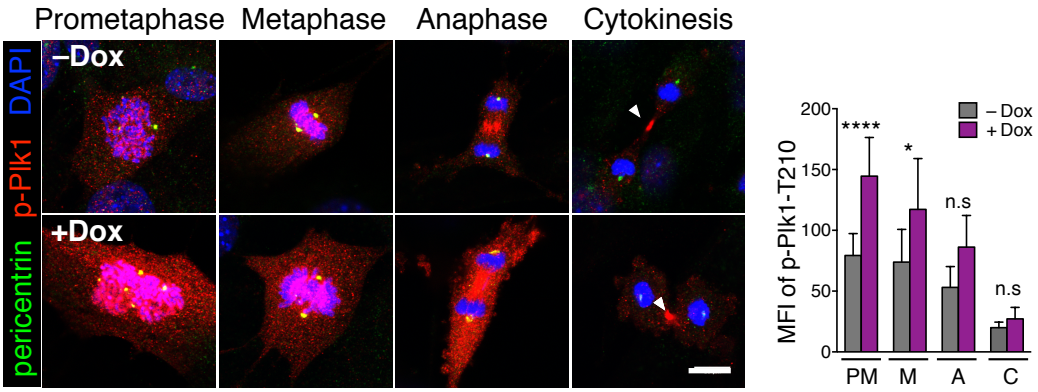

Figure 3.15: Immunofluorescence against p-Plk1 T210 and pericentrin in primary Plk1/Rosa26-rtTA MEFs after 24h on Dox. The histogram shows the quantification of mean fluorescence intensity (MFI) of p-Plk1T210 staining in the entire cell at each mitotic phase (Prometaphase (PM): –Dox n=9 cells; +Dox: n=11 cells; Metaphase (M): –Dox n=10 cells; +Dox: n=7 cells; Anaphase (A): –Dox n=11 cells; +Dox: n=9 cells; Cytokinesis (C): –Dox n=6 cells; +Dox: n=6 cells). ****, $p<0.0001$; *, $p<0.05$ (n=3 replicates); 1way ANOVA

The quantification of the signal revealed that there was a significant increase in the accumulation of Plk1-pT210 at prometaphase and metaphase in Plk1 over expressing MEFs. Although the other phases also showed a trend towards increased activated Plk1, this was not found to be significant (Figure 3.15). It was surprising that there was no increase in Plk1 activity during cytokinesis; especially since cytokinesis failure was identified as one of the major mechanisms that resulted in a genome-doubled progeny. It can be theorized that the cytokinesis failure was due to an effect caused by increased Plk1 activity in one of the earlier phases. However, it was now possible to associate the other major phenotype of lack of segregation, which resulted in mitotic exit prior to anaphase with the increase in activated Plk1 in prometaphase and metaphase.

To explore this line of thought, Plk1-pT210 signal localized at individual kinetochores during prometaphase was quantified. It was also necessary to show that Plk1

overexpression using this doxycycline inducible system did not affect the localization of the protein at the kinetochores. For this we performed immunofluorescence to confirm co-localization of Plk1-pT210 with a commonly used centromere marker, CREST (Figure 3.16b).

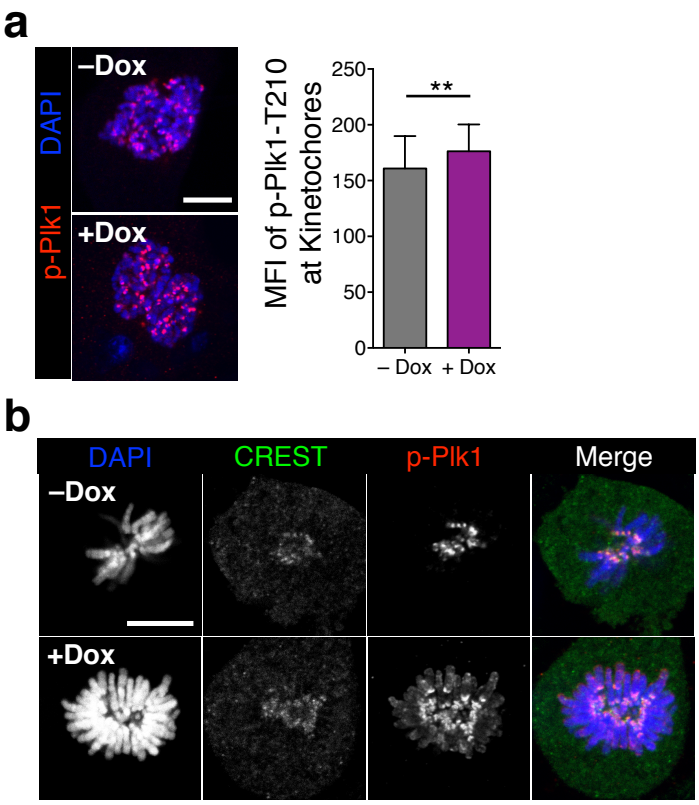

Figure 3.16: a) Immunofluorescence against p-Plk1T210 in primary Plk1/Rosa26-rtTA MEFs after 24h on Dox. The histogram shows the quantification of mean fluorescence intensity (MFI) of p-Plk1 T210 staining at individual kinetochores of cells in prometaphase (–Dox: n=51 kinetochores; +Dox: n=51 kinetochores) **, $p < 0.01$ (n=2 cells); Mann-Whitney test. b) Immunofluorescence against p-Plk1T210 and CREST in primary MEFs after 24h on Dox.

The results indicated that overexpression of Plk1 did not affect its localization to the kinetochore region and in line with the previous findings there was indeed an increase in localized Plk1 activity during prometaphase (Figure 3.16a).

3.14 The link to cohesion and the loss of Sgo1

The main function of Plk1 from prometaphase till anaphase that was relevant in producing the phenotype of non-segregation was the regulation of sister chromatid cohesion. It has already been shown that one of the main targets of Plk1 prior to metaphase is Sgo1, which is also known as the guardian of cohesion. This protein is localized at the centromeric region and protects cohesion prior to separation. When phosphorylated by Plk1 at the end of metaphase, Sgo1 is displaced from the kinetochores and cohesion is lost (Kitajima *et al.*, 2006). However, we theorized that

with the overexpression of Plk1 it is probable that the loss of cohesion is premature and cause the exit from mitosis without the occurrence of anaphase and chromosome segregation, resulting in a tetraploid progeny. To prove this hypothesis, we performed chromosome spreads of Plk1/Rosa26-rtTA MEFs treated with doxycycline for 48h. The analysis of the results indicated that with doxycycline induction, there was an increase in the percentage of spreads containing chromosomes with partial or complete loss of cohesion indicated by the separated arms and separated sister chromatids respectively (Figure 3.17).

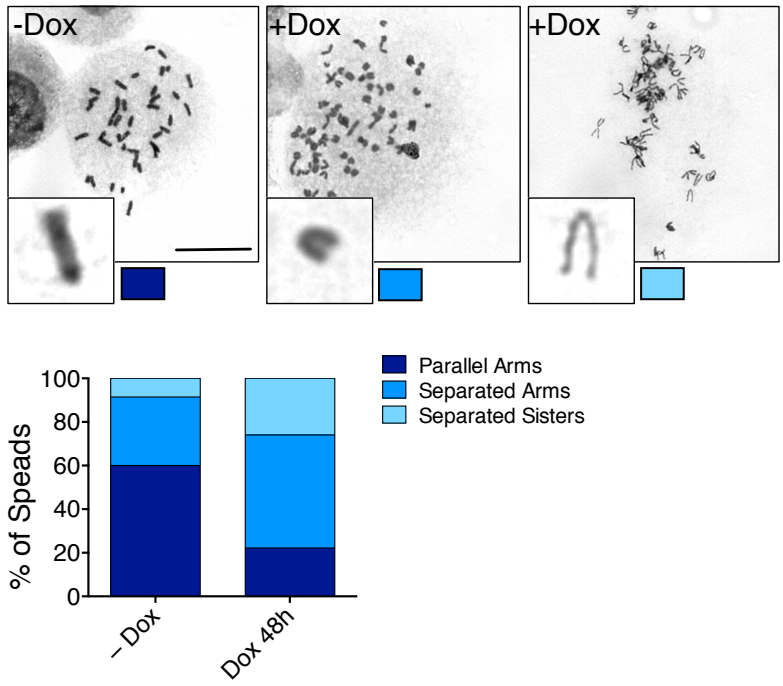

Figure 3.17: Chromosome spreads from Plk1/Rosa26-rtTA MEFs untreated or treated with Dox for 48h, where stained with giemsa and evaluated under the microscope. Chromosome cohesion was classified in three different status: "parallel arms" as readout of full chromatid cohesion (dark blue box), "separated arms" as readout of chromatid arm separation (mid blue) and "separated sisters" as readout of fully separated chromatids (light blue). (–Dox n=35 spreads; +Dox 48h: n=27 spreads). Scale bar 20 µm.

For verifying wether Plk1 overexpression affected Sgo1 localization, we performed immunofluroscence against Sgo1 and quantified the signal in prometaphase cells after 24h and 72h of doxycycline treatment.

The observations indicated that there was a decrease in overall Sgo1 staining in Plk1 overexpressing MEFs. In concurrence with reduction of Sgo1 there was also an increase in the percentage of cells where Sgo1 expression was diffused, when Plk1 overxepression was induced (Figure 3.18a). We also showed that Sgo1 localization was not affected in the controls by showing co-localization with centromere marker, CREST (Figure 3.18b). Taken as a whole this provides strong evidence in support of

the hypothesis that elevated levels of Plk1 leads to lack of chromosome segregation due to cohesion loss.

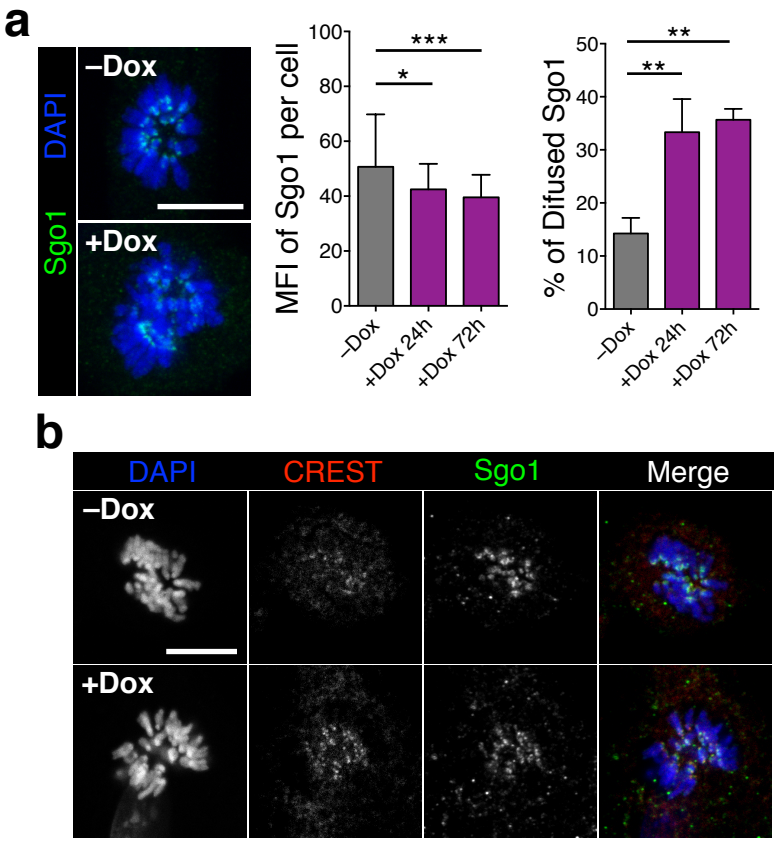

Figure 3.18: a) Immunofluorescence against p-Plk1 T210 and Sgo1 in primary Plk1/Rosa26-rtTA MEFs after 24h and 72h on Dox. The first histogram shows the quantification of mean fluorescence intensity (MFI) of Sgo1 staining in the entire cell at prometaphase (–Dox n=34 cells; +Dox 24h: n=38 cells; +Dox 72h: n=52 cells) *, $p<0.01$ (n=4 replicates); ***, $p<0.0001$ (n=5 replicates); 1way ANOVA. The second histogram shows the percentage of prometaphase cells with diffused Sgo1 staining (–Dox n=34 cells; +Dox 24h: n=38 cells; +Dox 72h: n=52 cells) **, $p<0.001$ (n=4 replicates); **, $p<0.001$ (n=5 replicates); 1way ANOVA. b) Immunofluorescence against Sgo1 and CREST in primary MEFs after 72h on Dox.

3.15 Secondary effects of polyploidy: extra centrosomes

Plk1 over expression resulted in genome doubled progeny as evidenced by results shown earlier; hence it was worth exploring the unavoidable repercussions this has on subsequent mitotic divisions. One of the main consequences associated with tetraploidy resulting from a failed mitotic division is the presence of extra centrosomes (Meraldi, Honda and Nigg, 2002). To explore this phenotype in Plk1 overexpressing MEFs, cells were stained with the centrosome marker gamma-tubulin and the percentage of mitotic cells with centrosomal defects was analyzed. MEFs with Plk1 overexpression showed a significant increase in cells with abnormal centrosome number, mainly attributed to supernumerary centrosomes (Figure 3.19).

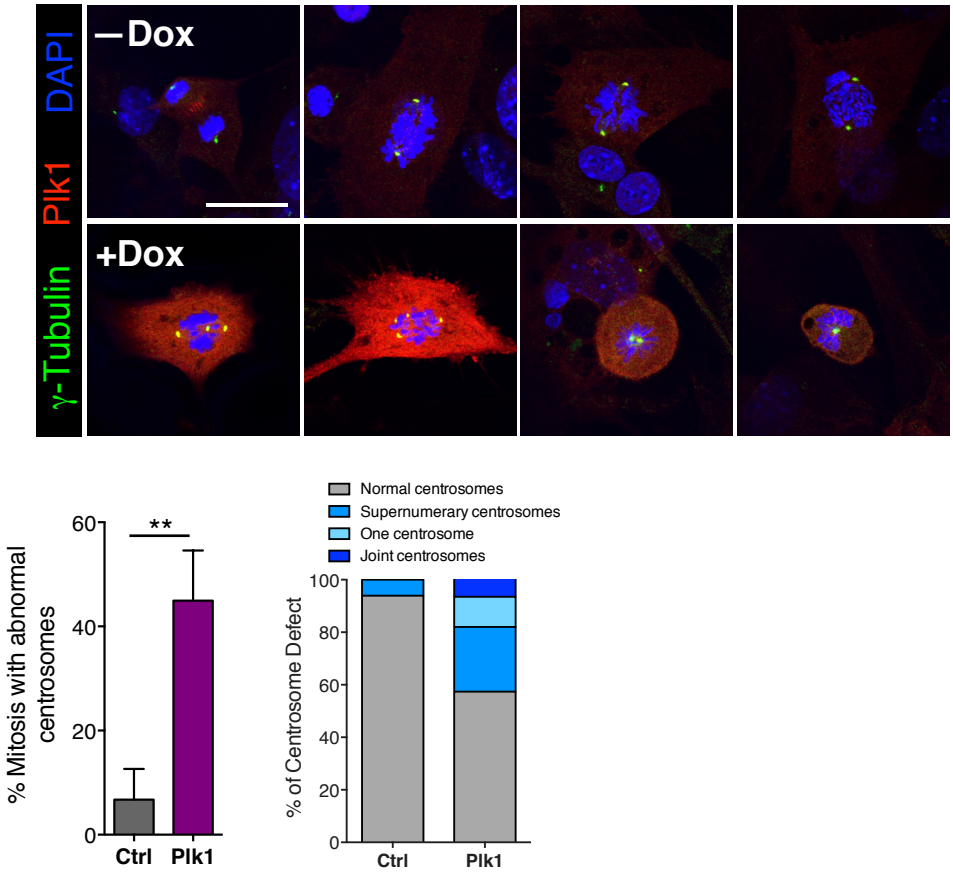

Figure 3.19: Immunofluorescence against Plk1 and gamma-tubulin in primary Plk1/Rosa26-rtTA MEFs after 24h on Dox. The histograms show the percentage of mitotic cells with centrosome abnormalities and the distribution of each type of centrosome defect. (Ctrl: n=49 mitotic cells; Plk1: n=61 mitotic cells) **, $p < 0.01$ (n=2 replicates); Mann-Whitney test.

Since Plk1 also plays a role in centrosome maturation and separation (Wang *et al.*, 2014), we needed to confirm that this phenotype was not caused directly by induced Plk1 overexpression. Centrosome maturation and separation happens in G1 and late G2 phases respectively. To find out if elevated levels of Plk1 affected this function; We stained Plk1 overexpressing MEFs with antibodies against Plk1-pT210 and pericentrin a centrosome marker and analyzed the staining intensity in interphase cells. Results indicated an increase in the amount of activated Plk1 localized at the separated centrosomes in G2 phase however there was no significant difference in the case of the joint centrosomes prior to that (Figure 3.20). This may suggest a possible effect of Plk1 overexpression on cells prior to entry into mitosis.

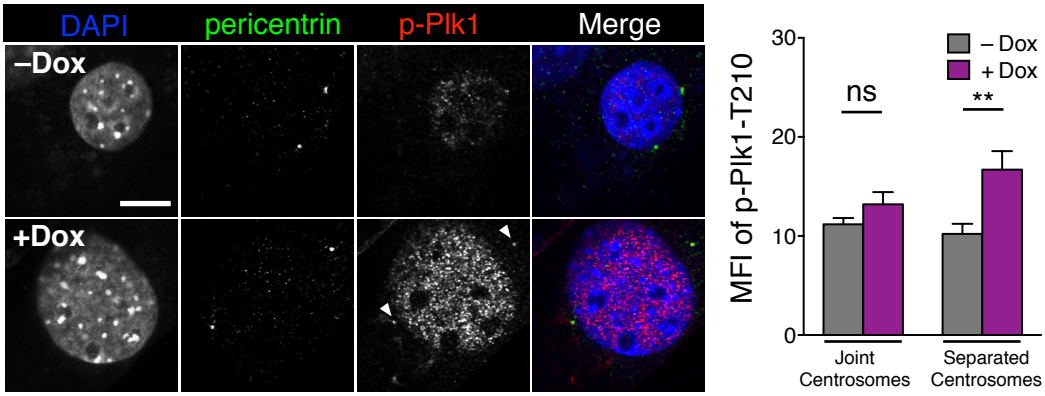

Figure 3.20: Immunofluorescence against p-Plk1 T210 and pericentrin in primary Plk1/Rosa26-rtTA MEFs after 24h on Dox. The histogram shows the quantification of mean fluorescence intensity (MFI) of p-Plk1T210 staining at the centrosomes during late G2 phase (separated) and rest of interphase (joint) (separated: –Dox: n=54 centrosomes; +Dox: n=34 centrosomes, joint: –Dox: n=88 centrosomes; +Dox: n=58 centrosomes) **, p<0.001 (n=2 replicates); 1way ANOVA.

Mammary Organoids

3.15 Mitotic aberrations and tetraploidization in Plk1 overexpressing mammary organoids

The MEFs provided an elegant yet simple *in vitro* system to understand the underlying mechanism behind the tetraploidization induced by Plk1 overexpression, however the aim of this study is to understand the consequences that elevated levels of Plk1 has on mammary tumorigenesis. If we were to extrapolate the results obtained by studying MEFs to mammary epithelial cells, we required an intermediate *in vitro* system of study, which more closely resembles our GEMMs. To address this, mammary organotypic cultures were directly derived from Plk1/MMTV-rtTA mice as described previously by (Jechlinger, Podsypanina and Varmus, 2009; Rowald *et al.*, 2016). To monitor the fate of epithelial cells after induction of Plk1, we performed time-lapse imaging of spheroid cultures 24h post induction of Plk1 with doxycycline. Nuclear content was visualized by genetic expression of H2B-GFP; images were captured every 5 minutes with the total session lasting 16h. Imaging time had to be limited to avoid any phototoxic effect to the cells.

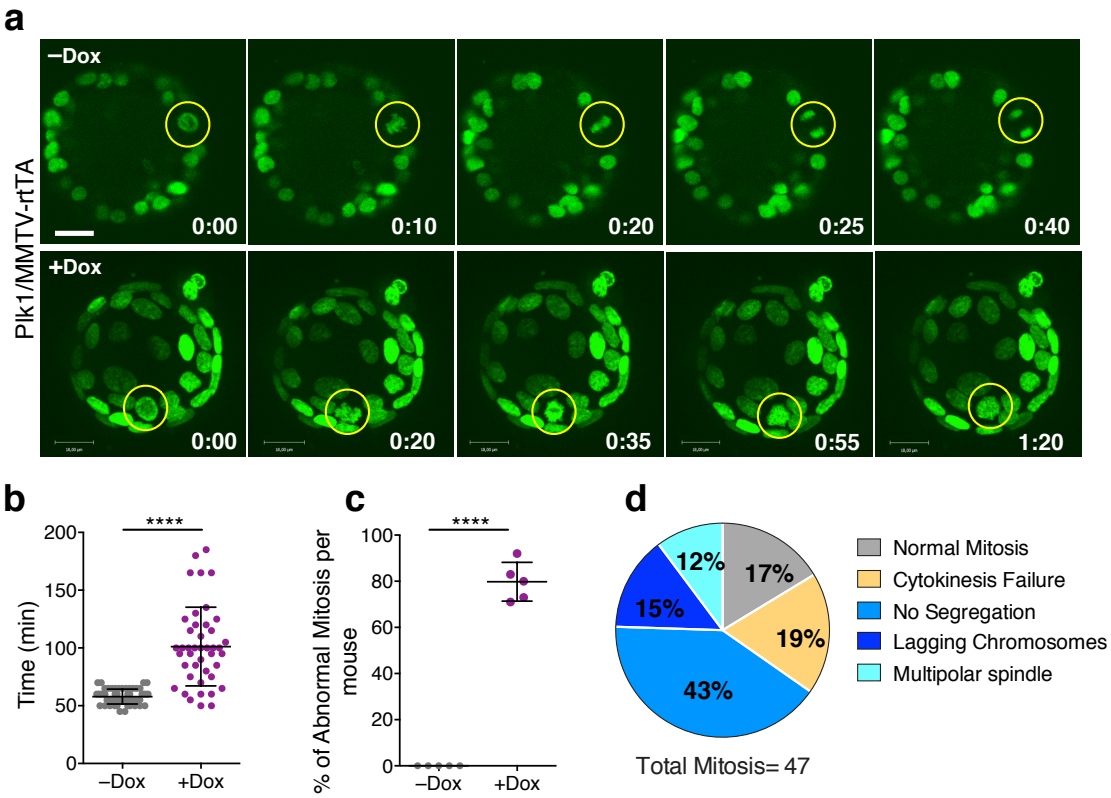

Figure 3.21: a) Time-lapse microscopy of Plk1/MMTV-rtTA mammary organoids untreated (upper panel) and after 24h on Dox (lower panel). Yellow circle indicates mitotic cells; H2B-GFP (green). Scale bar 18 µm. b) Duration of mitosis in the organoid cultures (–Dox: 57 cells; +Dox: 43 cells) ****, p<0.0001, Unpaired T-test. c) Percentage of mitotic errors per mouse; (–Dox: 57 cells from n=5 mice; +Dox: 47 cells from n=5 mice). ****, p<0.0001, Unpaired T-test. d) Outcome of mitotic cells overexpressing Plk1 after 36 hours.

The results were in congruence with the experiment conducted using MEFs except for a few exceptions. Mammary epithelial cells overexpressing Plk1 also resulted in a tetraploid progeny following a failed mitosis, however in this case the major cause was lack of chromosome segregation followed by exit prior to anaphase (43%). Contrastingly cytokinesis failure only contributed to 19% of all progeny becoming bi-nucleated. The epithelial cells overexpressing Plk1 also had a much higher percentage of abnormal mitosis whereas all control cells underwent normal division. Mitosis in the control cells lasted an average of 58min whereas the cells overexpressing Plk1 only managed to exit mitosis at an average of 101min (Figure 3.21a-d). This suggested mammary epithelial cells were more susceptible to the effects induced by Plk1 overexpression, thus providing a suitable explanation to the phenotypes observed *in vivo*.

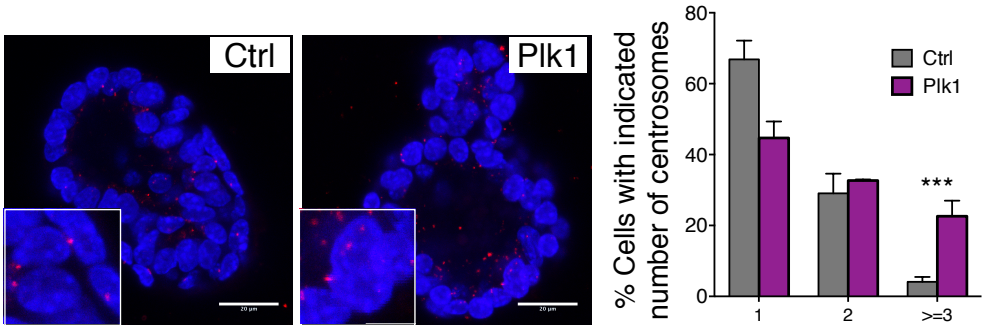

Figure 3.22: Immunofluorescence against pericentrin in mammary 3D cultures and quantification of percentage of cells per organoid with 1,2 or 3 centrosomes at 48h on doxycycline (Ctrl: n=204; Plk1: n=312) ***p < 0.001; Mann-Whitney Test. Number of animals: (CTRL: 3; Plk1: 3); Scale bar 20µm.

As was the case with the MEFs (Figure 3.19) and *in vivo* in the mammary gland (Figure 3.9b), tetraploidization due to Plk1 overexpression resulted in cells with supernumerary centrosomes as evidenced by immunofluorescence against pericentrin in mammary 3D cultures. Post induction of Plk1 expression, there was a significant increase in the percentage of cells per organoid with 3 or more centrosomes when compared to controls (Figure 3.22). These findings are in line with the *in vivo* and *in vitro* data presented earlier.

Summary of Results

The following were the main findings from this section:

- Overexpression of Plk1 does not lead to oncogenic transformation *in vivo*.
- Increased Plk1 levels lead to tumor suppression in Her2 and Kras driven murine breast cancer models.
- Tumors with elevated Plk1 show evidence of genome doubling and have increased levels of aneuploidy but they display a proliferative disadvantage.
- PLlk1 overexpression impairs chromosome segregation leading to tetraploidy and reduced proliferation *in vitro*.
- Tetraploidization results in mitotic aberrations and centrosome defects.
- Reduction of Sgo1, during prometaphase is responsible for loss of cohesion and possibly the lack of chromosome segregation.

Discussion

Plk1 has been the subject of great interest over the last few decades. Since it is a prominent kinase with several well-characterized functions in cell cycle regulation and the fact that it is overexpressed in many solid tumors made it a prime target for therapy (Eckerdt, Yuan and Strebhardt, 2005). However, following limited success in clinical trials using specific small molecule inhibitors, interest has waned on pursuing Plk1 as a potential target for therapy and it has been slowly relegated to the sidelines. Although vested interests have moved on to more promising treatments for the ever-evolving disease that is cancer, in this study we revisit Plk1 pondering if is worth considering as a therapeutic target and explore in detail the molecular mechanisms associated with Plk1 overexpression in mouse models of breast cancer. This work also elucidates the importance of such pre-clinical studies and usage of in vivo mouse models as a tool for validation, prior to further investment in large-scale clinical trials.

4.1 Tumor suppressive role of Plk1

Plk1 overexpression as part of the CIN70 signature is usually associated with bad prognosis and aggressive tumor phenotypes in human cancer (Carter *et al.*, 2006). Although Plk1 is overexpressed in several different tumors, its role in tumor initiation and development is yet to be determined (Cholewa, Liu and Ahmad, 2013). To address this question my collaborators from the Malumbres laboratory at the CNIO developed a tetracycline-inducible mouse model for studying the effects of Plk1 overexpression.

This mouse model uses a Tet-ON system where Plk1 expression is under the control of the Rosa26 ubiquitous promoter. When gene expression was induced throughout the animal with the addition of doxycycline, there was no significant increase in the incidence of tumors when compared to control animals (Section 3.1). Plk1 overexpression did not display any significant oncogenic potential in this mouse model. These results were largely surprising because experimental overexpression of other genes from the CIN70 signature led to spontaneous tumor development in those GEMMs (Sotillo *et al.*, 2007; Nam and Van Deursen, 2014).

Albeit the fact that Plk1 overexpression on its own was not sufficient to significantly increase neoplastic transformation, we postulated that it could cooperate with other oncogenic drivers and accelerate tumor onset. For the verification of this hypothesis, we established mouse models to study the effect of elevated levels of Plk1 in Kras or Her2 driven mammary tumorigenesis. In line with previous work from our lab and current literature, when mutant Kras ($Kras^{G12D}$) or Her2 is overexpressed mice develop palpable mammary gland tumors with complete penetrance and an average

latency of 155 and 98 days respectively. However, when Plk1 overexpression was combined with these potent oncogenes the ultimate result was an overwhelming tumor suppressive effect accompanied by a severe delay in tumor onset (Section 3.2).

These findings were in direct contradiction with the current consensus in the field as well as our initial hypothesis. Although the results obtained here do reinforce the major findings from a prior study conducted in our lab. This study clearly showed that overexpression of Mad2 also delayed mammary tumorigenesis in Kras and Her2 breast cancer models, as a consequence of prolonged mitotic arrest and increased apoptosis (Rowald *et al.*, 2016). Mad2 is also a member of the CIN70 signature, allowing us to hypothesize that overexpression of genes belonging to CIN70 can lead to tumor suppressive effects in a tissue specific context. Although several of the CIN genes have been shown to be tumor promotive, why is it in this case we observe the opposite effect? A major reasoning behind this is the tissue specific microenvironment which plays a pivotal role in tumorigenesis (Polyak and Kalluri, 2010). Another possible explanation would be the higher cell turnover rate in the breast compared to other tissues, owing to hormonal fluctuations caused by the estrus cycle (Visvader and Stingl, 2014).

The final result might be similar in both cases but the path taken to reach it could be vastly different, in other words, the mechanism by which Plk1 overexpression leads to tumor suppression can vary significantly from Mad2. Considering the distinct functions of both proteins this would be the likely scenario; it is thus important to determine the exact reasoning behind the tumor deterring phenotype caused by elevated levels of Plk1.

4.2 Genome Doubling in Tumors, a Consequence of Plk1 Overexpression?

In the introduction section, it was mentioned how whole genome doubling events are a relatively common occurrence during tumor development with a significant portion of these tumors still maintaining a near tetraploid karyotype (Dewhurst *et al.*, 2014). Hence, it is not surprising to observe tetraploid or polyploid cells also in mouse tumor models, which recapitulate human disease. Histological analysis of tumors from our mouse models however revealed a significant increase in the percentage of polyploid cells specifically in tumors overexpressing Plk1 compared to single oncogene tumors. These observations eluded at a probable role of the protein in inducing genome doubling (Section 3.3). A strong possibility considering the many roles the kinase plays during cell division and that tetraploidization mainly results from a failure in the cell division machinery (Davoli, de Lange and Lange, 2011).

A comprehensive analysis performed by our collaborator, Nicholas McGranahan (UCL), utilizing the TCGA BRCA dataset (cancergenome.nih.gov), consisting of 954

patient samples of breast invasive carcinoma revealed a significant correlation between Plk1 expression and genome doubling in these tumors (Figure 4.1). The results of this analysis firmly corroborate the observations made in our mouse tumor models. The distinct possibility that elevated levels of Plk1 causes genome doubling also in human tumors lends credibility to this study as well as emphasizes the importance of these GEMMs for further use in preclinical testing.

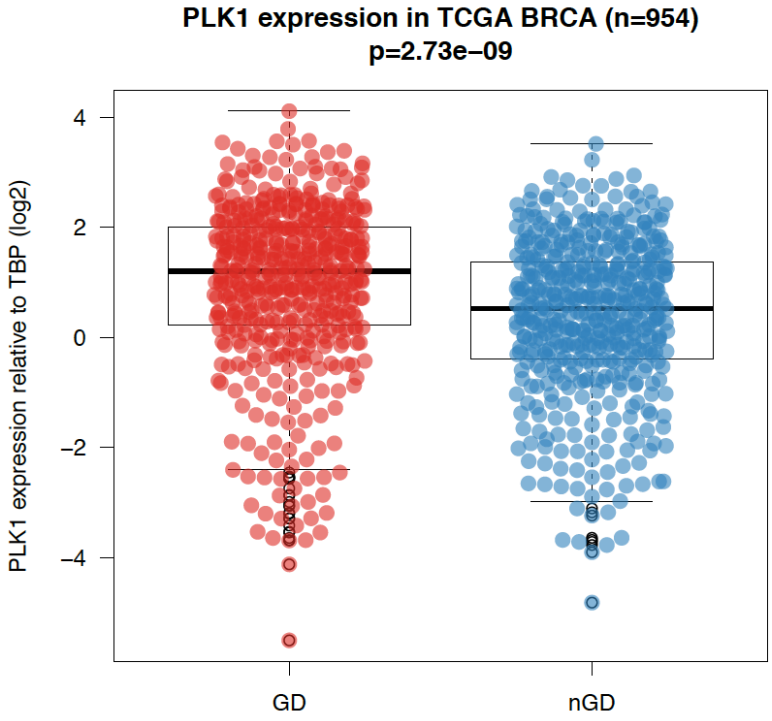

Figure 4.1: Plk1 expression relative to TATA box protein (TBP) in genome doubled (GD) and non-genome doubled (nGD) tumors of the TCGA BRCA dataset (n=954 breast invasive carcinoma patient samples). Analysis performed by Nicholas McGranahan (UCL) at the behest of personal correspondence (unpublished data).

Recent studies have shown that whole genome doubling promotes genomic instability, driving evolution and resulting in tumors with complex karyotypes. This is attributed to the fact that the whole genome doubling results in extra copies of all chromosomes and although these tetraploids are generally stable, their larger genomic pool allows them a higher tolerance towards chromosome gain or loss compared to diploid cells (Dewhurst *et al.*, 2014). The results obtained here are in concurrence with these findings. The tumors with elevated Plk1 levels indeed show a higher percentage of aneuploidy, which is a direct consequence of the genomic instability (Figure 3.4). It is also known that tumors with high levels of aneuploidy are more resilient to targeted therapy and can also be the cause of the increase in relapses post-treatment. The probability is high that this is also the case with these murine tumors overexpressing Plk1, although this could not be confirmed during this current project. We can, however, derive a conclusion because human tumors

overexpressing Plk1 generally show a poorer prognosis following primary treatment (kmplot.com).

The frequent occurrence of genome doubled cells in these tumors still does not provide an explanation for the tumor suppression caused by Plk1. Studies have shown that tetraploid cells, in general, have a reduced proliferative potential compared to their diploid counterparts and can be denoted as less fit. This reduced proliferation is attributed to a p53 dependent cell cycle (G1) arrest eventually leading to cell senescence or apoptosis. There is no specific tetraploid checkpoint in existence, meaning cells have no method of verifying correct chromosome number (Reviewed by Ganem and Pellman, 2007). However, following failed cell division several triggers, which cause cell cycle arrest and apoptosis, can activate p53, leading to the activation of the Hippo tumor suppressor pathway. The Hippo pathway is induced partially due to the presence of extra centrosomes in tetraploid cells which activates the kinase LATS2, causing stabilization of p53 and finally resulting in the inhibition of YAP and TAZ (Ganem *et al.*, 2014).

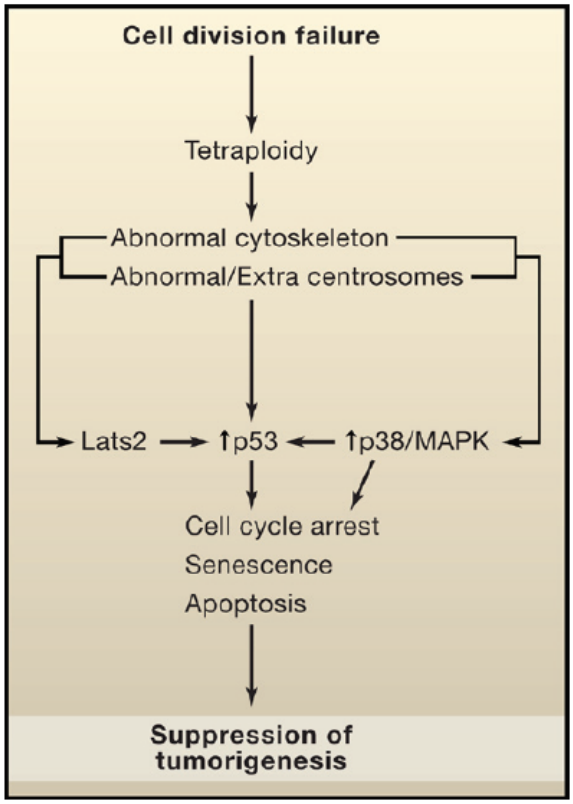

Figure 4.2: Triggers that lead the activation of p53 following failed cell division and the consequences (Ganem and Pellman, 2007).

The direct effector of p53 activation following these events is p21, which causes cell cycle arrest at the G1 phase. We questioned if this was observed also in the case of tumors overexpressing Plk1, which displayed a high percentage of polyploid cells. Immunohistochemistry analysis of p21 expression in Plk1 tumors showed a

significantly higher percentage of p21 positive cells in comparison to the single oncogene counterparts (Figure 3.5a). Moreover, tumors with elevated Plk1 also displayed a reduced proliferative potential as evidenced by PCNA staining. PCNA, which is a marker of cellular proliferation, was found to be expressed in a lesser percentage of cells in the Plk1 tumors compared to the Kras or Her2 tumors (Figure 3.5b). Considered together we conclude that tumors overexpressing Plk1 have increased karyotype complexity, elevated percentage of polyploid cells but also displays a decrease in proliferation due to p21 induced cell cycle arrest.

4.3 Effect of Plk1 prior to Tumor Initiation

Previously, we discussed the tumor suppressive role of Plk1 as well as the potential effects of Plk1 overexpression on the tumors themselves. However, it must be noted that the major phenotype observed in these cancer models is an overwhelming suppression of oncogenic transformation, with 90% of the Kras/Plk1 and 56% of the Her2/Plk1 animals not developing tumors (Section 3.1). Therefore, it was mandatory to study the effects of Plk1 overexpression on the mammary glands prior to tumor initiation.

We investigated two separate time points to further explore the role of Plk1 in early stages prior to tumor development. Mammary glands harvested 4 and 100 days post transgene induction showed a stable expression of Plk1 in all mouse models across both time points (Figure 3.6). Fold change of the Plk1 transgene as measured by qPCR was comparable to what was observed in human breast cancer cell lines, validating the efficacy of this model system in mimicking the human scenario (Figure 3.7).

The results obtained here indicated that Plk1 overexpression has a noticeable effect on the cellular morphology in the mammary gland as early as 4 days after induction. While the structure of the mammary acini itself remains unaffected, Plk1 caused an increase in the number of cells with a larger nuclear volume which is a clear indication of polyploidy (Figure 3.8). A recent study on mammary glands during lactation revealed the presence of naturally occurring polyploid cells arising from failed cytokinesis. The generation of these cells was dependent on overexpression of Aurora kinase-A as well as Plk1 and it was also suggested that this is a conserved mechanism essential for the lactation process. This was followed by the rapid clearance of these polyploid cells by apoptosis which occurred post pregnancy to prevent possible malignant transformation (Rios *et al.*, 2016).

Therefore, the mammary gland is an organ that inherently shows a higher tolerance towards polyploidy induced by Plk1 overexpression and has an intrinsic apoptotic mechanism that clears these cells, which is nonexistent in other tissues. This is one of the strong possibilities of how the transformation of polyploid cells is limited in

breast tissue. The other explanation is that irrespective of a tissue specific mechanism, just the presence of polyploid cells themselves can lead to cell cycle arrest, apoptosis and activation of tumor suppressor pathways, as discussed earlier. Despite polyploid cells being less fit they have an inherently higher potential for oncogenic transformation and by removing these cells from active cycling this effectively reduces the probability of transformation occurring in the tissue. In either case, the presence of polyploidy at an early stage provides an explanation for the strong tumor suppressive effect observed in the Plk1 expressing cohorts. This is further supported by the increase in apoptosis seen in the mammary gland cells over expressing Plk1 (Figure 3.9b).

4.4 Mechanisms inducing Polyploidy and their consequences

It was clear that the antiproliferative and tumor suppressive effects of Plk1 were a direct result of the induced polyploidy. With Plk1 partaking in different phases of the cell cycle (Petronczki, Lenart and Peters, 2008), it proved to be a challenge to pinpoint the exact function of the kinase that was responsible for the observed phenotype. It has long been known that Plk1 overexpression leads to tetraploidization, however, the mechanism causing it has not been concretely established (Meraldi, Honda and Nigg, 2002).

Time-lapse imaging of H2B-GFP labeled MEFs overexpressing Plk1 provided hints for unraveling this mechanism. In line with our *in vivo* results, the findings here indicated that over 60% of cells entering mitosis failed to complete cell division resulting in a genome doubled tetraploid progeny. Based on these observations, cell fate can be determined by one of these three possibilities. Either there was a failure in segregation due to impaired chromosome alignment followed by mitotic exit prior to anaphase resulting in a fused nucleus (27%) or cytokinesis failure occurred forming a bi-nucleated cell (38%). There were also a small percentage (7%) of cells that underwent mitotic regression after anaphase (Figure 3.11).

While we explored the broader implications of genome doubling and the roles it could play in tumorigenesis, what would be the immediate effects of tetraploidization at a cellular level? Plk1 overexpressing cells showed a high rate of erroneous division with most of the cells becoming tetraploid, one of the main consequences is these cells ending up with extra centrosomes as shown in section 3.14. Supernumerary centrosomes are a norm in tetraploid cells that result from failed cell division (Meraldi, Honda and Nigg, 2002) and the presence of extra centrosomes can lead to further mitotic aberrations such as multipolar spindles, lagging chromosomes and bridges as seen in Figure 3.9a. The schematic below (Figure 4.3) proposes a mechanism that explains how tetraploid cells with aberrant centrosomes that can bypass the p53 checkpoint result in aneuploid progeny during the following rounds of cell divisions. This model also lends more credibility to what

was discussed earlier. However, a recent study has shown that centrosome amplification caused directly by overexpression of Plk4 can act as a driving force for oncogenic transformation even with functional copies of p53 present (Levine *et al.*, 2017). Counter to this is the findings by Ganem *et al.* (2014) which revealed that extra centrosomes resulting from tetraploidization can indirectly cause p53 stabilization and the activation of tumor suppressive pathway. Possessing extra centrosomes can thus lead to both tumor promoting and suppressive effects depending on the situation. In the models described in this thesis, Plk1 overexpression in the mammary gland resulted in a tumor suppressive effect. In the future, it would be interesting to test whether overexpression of Plk1 together with other oncogenic drivers or even in combination with the absence of certain tumor suppressor genes will have the same effect. Finally, whether elevated levels of Plk1 in other tissues will result in similar outcomes is also worth exploring.

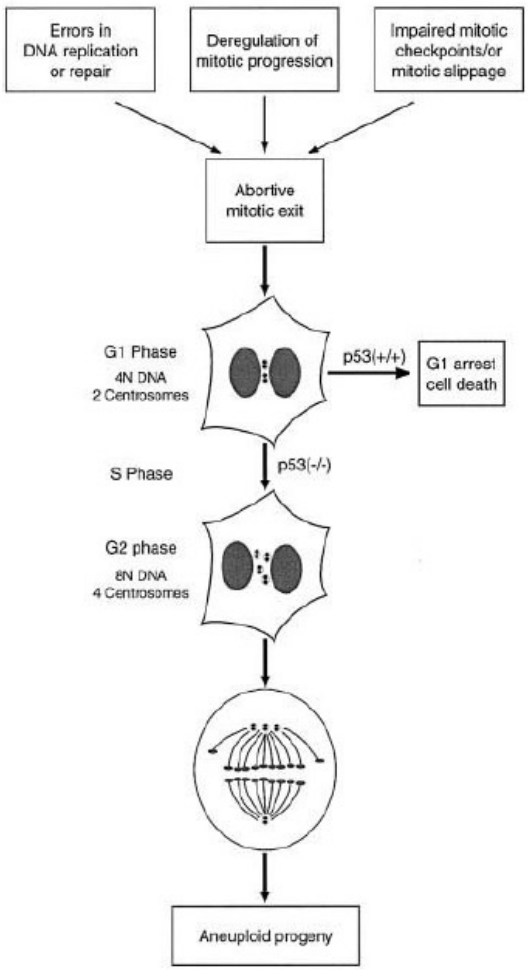

Figure 4.3: Impaired cell division results in tetraploid cells with supernumerary centrosomes. The proposed model indicates that upon failed mitotic exit cells carry an extra centrosome, these tetraploid cells are eliminated in a p53 wildtype background. The cells that evade this or possess a p53 mutation go through S phase producing a polyploid cell with 4 centrosomes, these cells are prone to aneuploidy (Meraldi, Honda and Nigg, 2002).

All evidence points out that the method of acquiring extra centrosomes in the MEFs is indeed failed mitosis. It could, however, be argued that the phenotype of supernumerary centrosomes could be directly caused by Plk1 overexpression. This argument is plausible because Plk1 is essential for centrosome maturation and separation (Nam and Van Deursen, 2014; Wang *et al.*, 2014), the overexpression of the kinase could affect these functions thereby indirectly affecting centrosome number. Our study found no evidence in support of this, elevated levels of activated pPlk1 at the centrosomes was only observed at the late G2 phase (Figure 3.17) after duplication and separation have already occurred, concluding that increase in Plk1 did not interfere with centrosome duplication.

4.5 Tetraploidization by Impaired Chromosome Segregation or Cytokinesis Failure

Even though cytokinesis failure was one of the major routes leading to tetraploidy in the MEFs, in this study we decided to emphasize on chromosome segregation failure and premature mitotic exit as the main mechanism driving polyploidy. There are a few reasons to justify this decision, first, there was a higher frequency of the lack of segregation phenotype compared to cytokinesis failure occurring when mitosis was monitored in mammary organoid cultures overexpressing Plk1 (Figure 3.18), the organoids are the more relevant system for this study. Second, there was a lack of evidence of bi-nucleation in vivo in the mouse breast tissue after induction of the transgene (data not shown). However, it can also be argued that bi-nucleated cells are an intermediate existence which will eventually result in polyploid cells during subsequent rounds of cell division (Meraldi, Honda and Nigg, 2002). The final reason is simply that lack of segregation and the premature mitotic exit happen before anaphase whereas cytokinesis failure can only occur during the final phase of mitosis, hence it can be reasoned that only the cells that escape the first phenotype can undergo cytokinesis failure making it a secondary effect.

To understand the causative factors that led to the failure of chromosome segregation, we first checked the localization and activation of Plk1 at different phases of mitosis. Plk1 activity was found to be increased in prometaphase and metaphase, 24 hours post induction (Figure 3.12), there was also more activated Plk1 localized specifically at the centromeric region during prometaphase (Figure 3.13a). One of the major functions of Plk1 that could be the cause of the observed phenotype is the role of the kinase in disrupting cohesion. Under normal conditions Plk1 is responsible for the phosphorylation of Sgo1 and removing the protein from its centromeric localization at anaphase, this allows separase to cleave cohesion and sister chromatids are pulled apart. The phosphatase PP2A which is an inhibitor of Plk1 function prevents this from happening prematurely (Kitajima *et al.*, 2006). However, with the overexpression of Plk1 in this model and the increase in accumulation of activated Plk1 at prometaphase, the loss of Sgo1 from the

centromeres can happen earlier thereby affecting cohesion. The results obtained also were in support, partial or complete cohesion loss was more frequently observed in chromosome spreads of MEFs with Plk1 overexpression (Figure 3.14). The decrease in Sgo1 expression, as well as diffused Sgo1 localization, was also observed in these cells, further reinforcing this hypothesis (Figure 3.15a). Loss of Sgo1 has been shown to cause mitotic arrest and premature mitotic exit (McGuinness *et al.*, 2005), these findings are in line with our findings which showed an increase in mitotic duration and exit without segregation (Figure 3.11a, d).

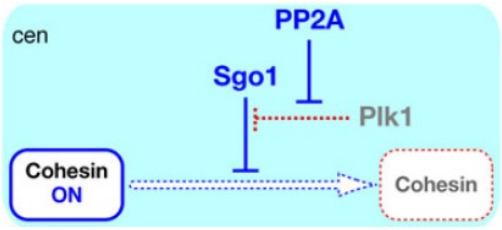

Figure 4.4: Plk1 mediates centromeric cohesion. In this model, Plk1 phosphorylates Sgo1 effectively removing it from the centromeres and exposes cohesion for degradation. PP2A counteracts this function of Plk1 (Shintomi and Hirano, 2010).

Even though we did not observe a significant increase in activated pPlk1 at the midbody during cytokinesis, this still warranted further study since bi-nucleation by cytokinesis failure was a prominent occurrence in Plk1 overexpressing MEFs and was also observed to a lesser degree in mammary 3D cultures. Experiments that were conducted to explore this phenotype are not a part of this dissertation, however, work carried out by our collaborators at the Malumbres laboratory offer a suitable explanation for this phenomenon. The results of that study confirmed the occurrence of aberrant cytokinesis in MEFs and concluded that over expression of Plk1 hindered the localization of the components belonging to the ESCRT complex, which was essential for abscission. One of the key components required for the assembly of this complex is Cep55, which is a target of Plk1. The phosphorylation of Cep55 by Plk1 prevents its localization to the midbody until the end of anaphase, when the levels of Plk1 drop at the end of anaphase Cep55 can properly localize and abscission can take place (Figure 4.5). When Plk1 is overexpressed the localization of Cep55 and TSG101, which is another component of the complex were both hindered and cytokinesis failure occurred due to a lack of abscission (unpublished data).

A combination of both mechanisms increased the accumulation of polyploid cells in Plk1 overexpressing *in vitro* culture systems. We can also extend these findings to provide a justification for the increase in polyploidy observed in the mouse models.

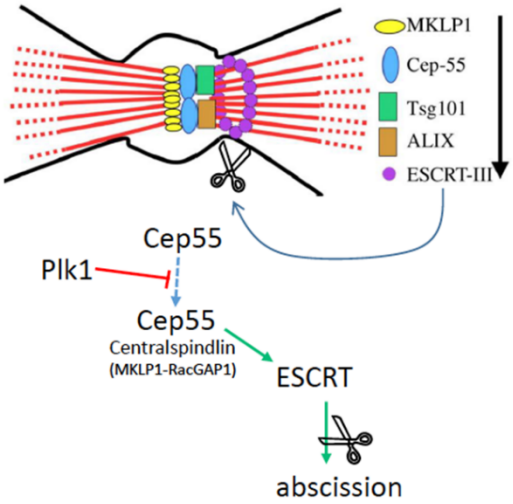

Figure 4.5: Assembly of ESCRT complex and the end of cytokinesis. Plk1 blocks the localization of Cep55 that is essential for the recruitment of the other components of the abscission complex. Figure adapted from (Carmena, 2012).

4.6 Concluding Remarks

During this project, we investigated the potential role of Plk1 to function as an oncogene in vivo and further explored if elevated levels of Plk1 could have any effect on tumor initiation in the presence of other more prominent oncogenic drivers. The results were quite contradictory to current consensus, Plk1 not only failed to function as an oncogene, in addition, it proved to be a potent tumor suppressor of Her2 and Kras driven breast cancer.

Further study using in vitro systems to explore the mechanism revealed that overexpression of Plk1 led to faulty chromosome segregation, with over 60% of all mitotic divisions resulting in tetraploid progeny, this also resulted in centrosomes defects among the said progeny with most of them possessing extra centrosomes. This phenotype was also well reflected in vivo in the mammary gland as well as observed in the tumors with high Plk1 expression. Though recent studies have shown that polyploidy, as well as centrosome amplification can have a prominent effect on promoting tumorigenesis, we have explored how the early stage induction of this phenotype can lead to a strong tumor suppressive effect in this context. Even though Plk1 lead to tumor suppression in most of the colony, the small percentage of tumors with elevated Plk1 levels displayed a complex karyotype thus further validating existing studies that state polyploidy allows for the tolerance of more CIN.

It must be stated that the conclusions drawn from this work are not necessarily in contradiction of using Plk1 inhibitors for targeted therapy. Although Plk1 overexpression in this context acted as a tumor suppressor, when induced at a later stage of tumor development it could have the opposite effect, possibly after the loss of the tumor suppressor p53. Even if this were not to be the case, the inhibition of Plk1 in human tumors could still have an anti-tumor effect simply due to the importance of the kinase during cell division. This study is directed to elucidate the molecular mechanisms associated with Plk1 overexpression and speculates how this

knowledge could be beneficial for gaining a better understanding for the proper use of Plk1 specific inhibitors during treatment.

References

Ando, K. *et al.* (2004) 'Polo-like kinase 1 (Plk1) inhibits p53 function by physical interaction and phosphorylation', *Journal of Biological Chemistry*, 279(24), pp. 25549–25561. doi: 10.1074/jbc.M314182200.

Archambault, V., Lépine, G. and Kachaner, D. (2015) 'Understanding the Polo Kinase machine.', *Oncogene*, 34(November 2014), pp. 1–9. doi: 10.1038/onc.2014.451.

Ashford, N. A. *et al.* (2015) 'Cancer risk : Role of environment Cancer risk : Tumors excluded Cancer risk : Role of chance overstated Cancer risk : Prevention is crucial Cancer risk : Many factors contribute', 347(160).

Boxer, R. B. *et al.* (2004) 'Lack of sustained regression of c-MYC-induced mammary adenocarcinomas following brief or prolonged MYC inactivation', *Cancer Cell*, 6(6), pp. 577–586. doi: 10.1016/j.ccr.2004.10.013.

Burkard, M. E. *et al.* (2007) 'Chemical genetics reveals the requirement for Polo-like kinase 1 activity in positioning RhoA and triggering cytokinesis in human cells.', *Proceedings of the National Academy of Sciences of the United States of America*, 104(11), pp. 4383–8. doi: 10.1073/pnas.0701140104.

Burstein, H. J. *et al.* (2014) 'Adjuvant endocrine therapy for women with hormone receptor-positive breast cancer: American Society of Clinical Oncology clinical practice guideline focused update', *Journal of Clinical Oncology*, 32(21), pp. 2255–2269. doi: 10.1200/JCO.2013.54.2258.

De Cárcer, G., Manning, G. and Malumbres, M. (2011) 'From Plk1 to Plk5: Functional evolution of Polo-like kinases', *Cell Cycle*, 10(14), pp. 2255–2262. doi: 10.4161/cc.10.14.16494.

Carmena, M. (2012) 'Abscission checkpoint control: stuck in the middle with Aurora B', *Open Biology*, 2(7), pp. 120095–120095. doi: 10.1098/rsob.120095.

Carter, S. L. *et al.* (2006) 'A signature of chromosomal instability inferred from gene expression profiles predicts clinical outcome in multiple human cancers', *Nat Genet*, 38(9), pp. 1043–1048. doi: 10.1038/ng1861.

Casenghi M, Meraldi P, Weinhart U, Duncan PI, Körner R, Nigg, E. (2003) 'Polo-like kinase 1 regulates Nlp, a centrosome protein involved in microtubule nucleation.', *Dev Cell*, 5, pp. 113–125.

Cheng, K. Y. *et al.* (2003) 'The crystal structure of the human polo-like kinase-1 polo box domain and its phospho-peptide complex', *EMBO Journal*, 22(21), pp. 5757–5768. doi: 10.1093/emboj/cdg558.

Cho, A., Haruyama, N. and Kulkarni, A. (2009) 'Generation of Transgenic Mice', *Curr Protoc Cell Biol.* doi: 10.1002/0471143030.cb1911s42.Generation.

Choi, M. *et al.* (2015) 'Polo-like kinase 1 inhibitor BI2536 causes mitotic catastrophe following activation of the spindle assembly checkpoint in non-small cell lung cancer cells', *Cancer Letters*, 357(2), pp. 591–601. doi: 10.1016/j.canlet.2014.12.023.

Cholewa, B. D., Liu, X. and Ahmad, N. (2013) 'The role of polo-like kinase 1 in carcinogenesis: Cause or consequence?', *Cancer Research*, 73(23), pp. 6848–6855. doi: 10.1158/0008-

5472.CAN-13-2197.

Crockford, A. *et al.* (2017) 'Cyclin D mediates tolerance of genome-doubling in cancers with functional p53', *Annals of Oncology*, 28(1), pp. 149–156. doi: 10.1093/annonc/mdw612.

Davoli, T., de Lange, T. and Lange, T. (2011) 'The Causes and Consequences of Polyploidy in Normal Development and Cancer', *Annu. Rev. Cell Dev. Biol.*, 27(1), pp. 585–610. doi: 10.1146/annurev-cellbio-092910-154234.

Dewhurst, S. M. *et al.* (2014) 'Tolerance of whole- genome doubling propagates chromosomal instability and accelerates cancer genome evolution', *Cancer Discovery*, 4(2), pp. 175–185. doi: 10.1158/2159-8290.CD-13-0285.

Eckerdt, F., Yuan, J. and Strebhardt, K. (2005) 'Polo-like kinases and oncogenesis.', *Oncogene*, 24(2), pp. 267–276. doi: 10.1038/sj.onc.1208273.

Elowe, S. *et al.* (2007) 'on BubR1 regulates the stability of kinetochore – microtubule interactions', *Genes & Development*, pp. 2205–2219. doi: 10.1101/gad.436007.2004.

Fujiwara, T. *et al.* (2005) 'Cytokinesis failure generating tetraploids promotes tumorigenesis in p53-null cells.', *Nature*, 437(7061), pp. 1043–7. doi: 10.1038/nature04217.

Ganem, N. J. *et al.* (2014) 'Cytokinesis failure triggers hippo tumor suppressor pathway activation', *Cell*, 158(4), pp. 833–848. doi: 10.1016/j.cell.2014.06.029.

Ganem, N. J. and Pellman, D. (2007) 'Limiting the Proliferation of Polyploid Cells', *Cell*, 131(3), pp. 437–440. doi: 10.1016/j.cell.2007.10.024.

Godek, K. M. *et al.* (2016) 'Chromosomal instability affects the tumorigenicity of glioblastoma tumor-initiating cells', *Cancer Discovery*, 6(5), pp. 532–545. doi: 10.1158/2159-8290.CD-15-1154.

Goel, S. *et al.* (2016) 'Overcoming Therapeutic Resistance in HER2-Positive Breast Cancers with CDK4/6 Inhibitors', *Cancer Cell*. Elsevier Inc., 29(3), pp. 255–269. doi: 10.1016/j.ccell.2016.02.006.

Gutteridge, R. E. A. *et al.* (2016) 'Plk1 Inhibitors in Cancer Therapy: From Laboratory to Clinics', *Molecular Cancer Therapeutics*, pp. 1–9. doi: 10.1158/1535-7163.MCT-15-0897.

Hartwell, L. H. *et al.* (1973) 'Genetic control of the cell division cycle in yeast: V. Genetic analysis of cdc mutants', *Genetics*, 74(2), pp. 267–286. doi: 74(2): 267–286.

Hornig, N. C. D. and Uhlmann, F. (2004) 'Preferential cleavage of chromatin-bound cohesin after targeted phosphorylation by Polo-like kinase.', *The EMBO journal*, 23(15), pp. 3144–3153. doi: 10.1038/sj.emboj.7600303.

Hu, D. *et al.* (2007) 'CDK11(p58) is required for the maintenance of sister chromatid cohesion.', *Journal of cell science*, 120(Pt 14), pp. 2424–2434. doi: 10.1242/jcs.007963.

Ito, Y. *et al.* (2004) 'Polo-like kinase 1 overexpression is an early event in the progression of papillary carcinoma', *British journal of cancer*, 86(6), pp. 912–916. doi: 10.1038/sj.bjc.6600172.

Jechlinger, M., Podsypanina, K. and Varmus, H. (2009) 'Regulation of transgenes in three-dimensional cultures of primary mouse mammary cells demonstrates oncogene dependence and identifies cells that survive deinduction', *Genes and Development*, 23(14), pp. 1677–1688. doi: 10.1101/gad.1801809.

Kim, H. *et al.* (2014) 'Centralspindlin assembly and 2 phosphorylations on MgcRacGAP by Polo-like kinase 1 initiate Ect2 binding in early cytokinesis', *Cell Cycle*, 13(18), pp. 2952–2961. doi: 10.4161/15384101.2014.947201.

Kirkland, J. (1966) 'COMPARATIVE STUDY OF HISTOLOGIC AND', *Cancer*.

Kishi, K. *et al.* (2009) 'Functional dynamics of Polo-like kinase 1 at the centrosome.', *Molecular and cellular biology*, 29(11), pp. 3134–3150. doi: 10.1128/MCB.01663-08.

Kitajima, T. S. *et al.* (2006) 'Shugoshin collaborates with protein phosphatase 2A to protect cohesin.', *Nature*, 441(7089), pp. 46–52. doi: 10.1038/nature04663.

Lee, K. S. *et al.* (1998) 'Mutation of the polo-box disrupts localization and mitotic functions of the mammalian polo kinase Plk.', *Proceedings of the National Academy of Sciences of the United States of America*, 95(16), pp. 9301–6. doi: 10.1073/pnas.95.16.9301.

Lénárt, P. *et al.* (2007) 'The Small-Molecule Inhibitor BI 2536 Reveals Novel Insights into Mitotic Roles of Polo-like Kinase 1', *Current Biology*, 17(4), pp. 304–315. doi: 10.1016/j.cub.2006.12.046.

Levine, M. S. *et al.* (2017) 'Centrosome Amplification Is Sufficient to Promote Spontaneous Tumorigenesis in Mammals', *Developmental Cell*. Elsevier Inc., 40(3), p. 313–322.e5. doi: 10.1016/j.devcel.2016.12.022.

Liu, X. S. *et al.* (2010) 'Polo-like kinase 1 phosphorylation of G2 and S-phase-expressed 1 protein is essential for p53 inactivation during G2 checkpoint recovery.', *EMBO reports*. Nature Publishing Group, 11(8), pp. 626–32. doi: 10.1038/embor.2010.90.

López-García, C. *et al.* (2017) 'BCL9L Dysfunction Impairs Caspase-2 Expression Permitting Aneuploidy Tolerance in Colorectal Cancer', *Cancer Cell*, 31(1), pp. 79–93. doi: 10.1016/j.ccell.2016.11.001.

Losada, A., Hirano, M. and Hirano, T. (2002) 'Cohesin release is required for sister chromatid resolution, but not for condensin-mediated compaction, at the onset of mitosis', *Genes and Development*, 16(23), pp. 3004–3016. doi: 10.1101/gad.249202.

McGuinness, B. E. *et al.* (2005) 'Shugoshin prevents dissociation of cohesin from centromeres during mitosis in vertebrate cells', *PLoS Biology*, 3(3), pp. 0433–0449. doi: 10.1371/journal.pbio.0030086.

Medema, R. H., Lin, C.-C. and Yang, J. C.-H. (2011) 'Polo-like kinase 1 inhibitors and their potential role in anticancer therapy, with a focus on NSCLC.', *Clin Cancer Res*, 17(20), pp. 6459–6466. doi: 10.1158/1078-0432.CCR-11-0541.

Menezes, M. E. *et al.* (2014) *Genetically engineered mice as experimental tools to dissect the critical events in breast cancer*, *Advances in cancer research*. doi: 10.1016/B978-0-12-800249-0.00008-1.

Meraldi, P., Honda, R. and Nigg, E. A. (2002) 'Aurora-A overexpression reveals tetraploidization as a major route to centrosome amplification in p53-/- cells', *EMBO Journal*, 21(4), pp. 483–492. doi: 10.1093/emboj/21.4.483.

Moasser, M. M. and Krop, I. E. (2015) 'The evolving landscape of her2 targeting in breast cancer', *JAMA Oncology*, 1(8), pp. 1154–1161. Available at: http://dx.doi.org/10.1001/jamaoncol.2015.2286.

Moody, S. E. *et al.* (2002) 'Conditional activation of Neu in the mammary epithelium of transgenic mice results in reversible pulmonary metastasis', *Cancer Cell*, 2(6), pp. 451–461.

doi: 10.1016/S1535-6108(02)00212-X.

Nam, H.-J. and Van Deursen, J. M. (2014) 'Cyclin B2 and p53 control proper timing of centrosome separation', *Nature cell biology*, 16(6), pp. 535–546. doi: 10.1038/ncb2952.

Nelson, H. D. *et al.* (2009) 'Screening for breast cancer: systematic evidence review update for the U. S. preventive services task force', *Ann Intern Med*, 151(74), pp. 727–742.

Neve, R. M. *et al.* (2009) 'A collection of breast cancer cell lines for the study of functionally', *Cancer Cell*, 10(6), pp. 515–527. doi: 10.1016/j.ccr.2006.10.008.A.

O'Hagan, R. C. and Heyer, J. (2011) 'KRAS Mouse Models: Modeling Cancer Harboring KRAS Mutations', *Genes & Cancer*, 2(3), pp. 335–343. doi: 10.1177/1947601911408080.

Perera, D. and Taylor, S. S. (2010) 'Sgo1 establishes the centromeric cohesion protection mechanism in G2 before subsequent Bub1-dependent recruitment in mitosis.', *Journal of cell science*, 123(Pt 5), pp. 653–659. doi: 10.1242/jcs.059501.

Petersen, O. W. *et al.* (1992) 'Interaction with basement membrane serves to rapidly distinguish growth and differentiation pattern of normal and malignant human breast epithelial cells.', *Proceedings of the National Academy of Sciences of the United States of America*, 89(19), pp. 9064–9068. doi: 10.1073/pnas.90.6.2556c.

Petronczki, M., Lenart, P. and Peters, J. M. (2008) 'Polo on the Rise-from Mitotic Entry to Cytokinesis with Plk1', *Developmental Cell*, 14(5), pp. 646–659. doi: 10.1016/j.devcel.2008.04.014.

Podsypanina, K. *et al.* (2008) 'Oncogene cooperation in tumor maintenance and tumor recurrence in mouse mammary tumors induced by Myc and mutant Kras.', *Proceedings of the National Academy of Sciences of the United States of America*, 105(13), pp. 5242–7. doi: 10.1073/pnas.0801197105.

Polyak, K. and Kalluri, R. (2010) 'The role of the microenvironment in mammary gland development and cancer.', *Cold Spring Harb Perspect Biol*, 2(11), p. a003244. doi: 10.1101/cshperspect.a003244.

Pylayeva-Gupta, Y., Grabocka, E. and Bar-Sagi, D. (2011) 'RAS oncogenes: weaving a tumorigenic web', *Nature reviews. Cancer*. Nature Publishing Group, 11(11), pp. 761–74. doi: 10.1038/nrc3106.

Rexer, B. N. and Arteaga, C. L. (2012) 'Intrinsic and acquired resistance to HER2-targeted therapies in HER2 gene-amplified breast cancer: mechanisms and clinical implications.', *Critical reviews in oncogenesis*, 17(1), pp. 1–16. doi: 10.1615/CritRevOncog.v17.i1.20.

Rios, A. C. *et al.* (2016) 'Essential role for a novel population of binucleated mammary epithelial cells in lactation.', *Nature communications*. Nature Publishing Group, 7, p. 11400. doi: 10.1038/ncomms11400.

Rowald, K. *et al.* (2016) 'Negative Selection and Chromosome Instability Induced by Mad2 Overexpression Delay Breast Cancer but Facilitate Oncogene-Independent Outgrowth', *Cell Reports*. The Authors, 15(12), pp. 2679–2691. doi: 10.1016/j.celrep.2016.05.048.

Saini, K. S. *et al.* (2012) 'Role of the multidisciplinary team in breast cancer management: Results from a large international survey involving 39 countries', *Annals of Oncology*, 23(4), pp. 853–859. doi: 10.1093/annonc/mdr352.

Seki, A., Coppinger, J. and Jang, C. (2008) 'Bora and Aurora A Cooperatively Activate Plk1 and Control the Entry into Mitosis', *Science (New York,* 320(5883), pp. 1655–1658. doi:

10.1126/science.1157425.Bora.

Shamir, E. R. and Ewald, A. J. (2014) 'Three-dimensional organotypic culture: experimental models of mammalian biology and disease.', *Nature reviews. Molecular cell biology*. Nature Publishing Group, 15(10), pp. 647–64. doi: 10.1038/nrm3873.

Shintomi, K. and Hirano, T. (2010) 'Sister chromatid resolution: A cohesin releasing network and beyond', *Chromosoma*, 119(5), pp. 459–467. doi: 10.1007/s00412-010-0271-z.

Siegel, R., Miller, K. and Jemal, A. (2015) 'Cancer statistics , 2015 .', *CA Cancer J Clin*, 65(1), p. 29. doi: 10.3322/caac.21254.

Sotillo, R. *et al.* (2007) 'Mad2 Overexpression Promotes Aneuploidy and Tumorigenesis in Mice', *Cancer Cell*, 11(1), pp. 9–23. doi: 10.1016/j.ccr.2006.10.019.

Steegmaier, M. *et al.* (2007) 'BI 2536, a Potent and Selective Inhibitor of Polo-like Kinase 1, Inhibits Tumor Growth In Vivo', *Current Biology*, 17(4), pp. 316–322. doi: 10.1016/j.cub.2006.12.037.

Sunkel, C. E. and Glover, D. M. (1988) 'polo, a mitotic mutant of Drosophila displaying abnormal spindle poles.', *Journal of cell science*, 89 (Pt 1), pp. 25–38. doi: 10.1016/j.

Toyoshima-Morimoto, F. *et al.* (2001) 'Polo-like kinase 1 phosphorylates cyclin B1 and targets it to the nucleus during prophase.', *Nature*, 410(March), pp. 215–220. doi: 10.1038/35065617.

Visvader, J. E. and Stingl, J. (2014) 'Mammary stem cells and the differentiation hierarchy : current status and perspectives', pp. 1143–1158. doi: 10.1101/gad.242511.114.targeted.

Wang, G. *et al.* (2014) 'The role of mitotic kinases in coupling the centrosome cycle with the assembly of the mitotic spindle.', *Journal of cell science*, 127(Pt 19), pp. 4111–22. doi: 10.1242/jcs.151753.

Wang, T. C. *et al.* (1994) 'Mammary hyperplasia and carcinoma in MMTV-cyclin D1 transgenic mice.', *Nature*, 369, pp. 669–671. doi: 10.1038/369669a0.

Van De Weerdt, B. C. M. and Medema, R. H. (2006) 'Polo-like kinases: A team in control of the division', *Cell Cycle*, 5(8), pp. 853–864. doi: 10.4161/cc.5.8.2692.

Appendix

Publications

The following manuscript contains most of the results presented in this thesis:

Plk1 overexpression suppresses tumor development by inducing chromosomal instability

Guillermo de Cárcer[1,#,*], **Sharavan Vishaan Venkateswaran[2,#]**, Aicha El Bakkali[1], Kalman Somogyi[2], Konstantina Rowald[2], Pablo Montañes[1], Manuel Sanclemente[1], Beatriz Escobar[1], Alba de Martino[3], Marcos Malumbres[1,*,&] and Rocío Sotillo[2,*,&]

[1] *Cell Division and Cancer Group, Spanish National Cancer Research Centre (CNIO), Melchor Fernández Almagro 3, E-28029 Madrid, Spain*
[2] *Division of Molecular Thoracic Oncology, German Cancer Research Center (DKFZ), Im Neuenheimer Feld 280, 69120 Heidelberg, Germany; and Translational Lung Research Center Heidelberg (TRLC), German Center for Lung Research (DZL), Germany*
[3] *Histopathology Unit, Spanish National Cancer Research Centre (CNIO)*

 # These authors contributed equally to this work.
& These authors contributed equally to this work.

Status: Submitted to Nature Communications

The following manuscript contains contributions not detailed in this thesis:

Cellular Prion Protein PrP^C and Ecto-5'-Nucleotidase Are Markers of the Cellular Stress Response to Aneuploidy

Patrícia H. Domingues, Lalitha S.Y. Nanduri, Katarzyna Seget, **Sharavan V. Venkateswaran**, David Agorku, Cristina Viganó, Conrad von Schubert, Erich A. Nigg, Charles Swanton, Rocío Sotillo, Andreas Bosio, Zuzana Storchová and Olaf Hardt

Cancer Research; Published OnlineFirst April 4, 2017;

DOI: 10.1158/0008-5472.CAN-16-3052